LBNL-42158

ERNEST ORLANDO LAWRENCE BERKELEY NATIONAL LABORATORY

Using TRINET for Simulating Flow and Transport in Porous Media

Julie Najita and Christine Doughty

Earth Sciences Division

August 1998

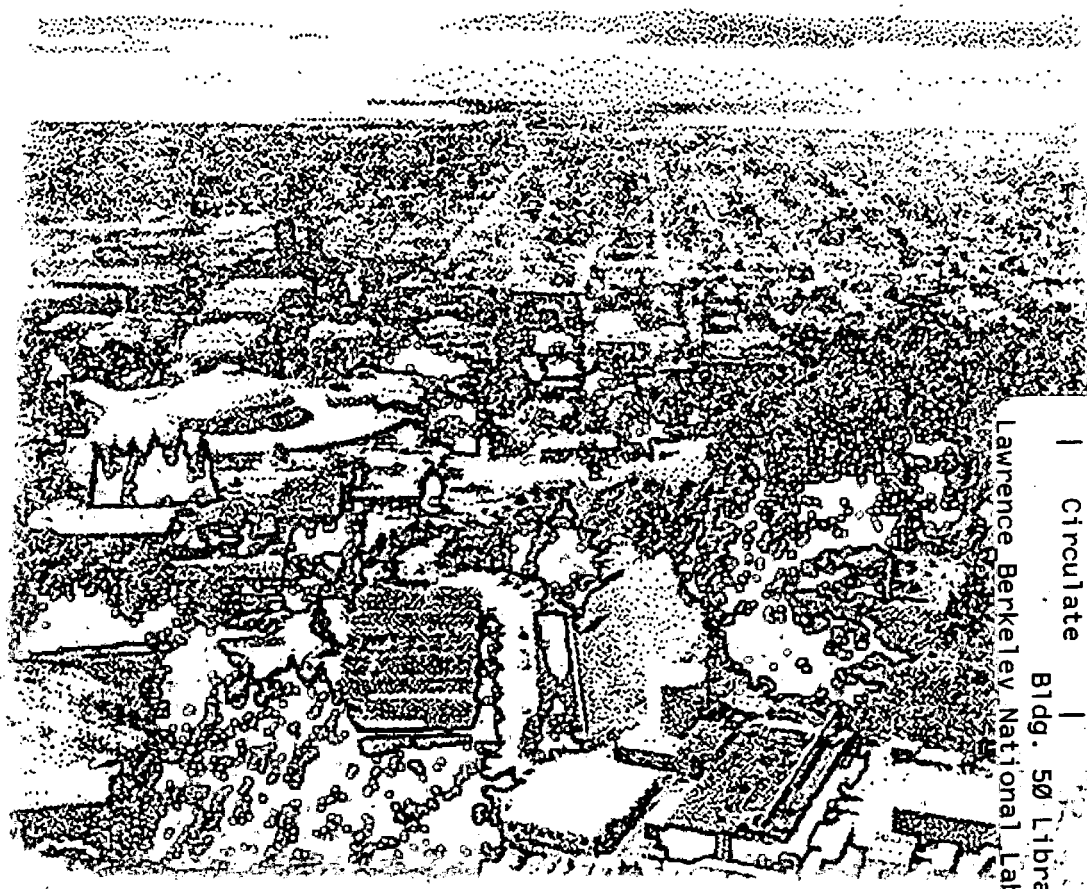

REFERENCE COPY
Does Not
Circulate
Bldg. 50 Library - Ref.
Lawrence Berkeley National Laboratory
Copy 1
LBNL-42158

DISCLAIMER

This document was prepared as an account of work sponsored by the United States Government. While this document is believed to contain correct information, neither the United States Government nor any agency thereof, nor the Regents of the University of California, nor any of their employees, makes any warranty, express or implied, or assumes any legal responsibility for the accuracy, completeness, or usefulness of any information, apparatus, product, or process disclosed, or represents that its use would not infringe privately owned rights. Reference herein to any specific commercial product, process, or service by its trade name, trademark, manufacturer, or otherwise, does not necessarily constitute or imply its endorsement, recommendation, or favoring by the United States Government or any agency thereof, or the Regents of the University of California. The views and opinions of authors expressed herein do not necessarily state or reflect those of the United States Government or any agency thereof or the Regents of the University of California.

LBNL-42158

Using TRINET for Simulating Flow and Transport in Porous Media

Julie Najita and Christine Doughty

Earth Sciences Division
Ernest Orlando Lawrence Berkeley National Laboratory
Berkeley, CA 94720

August 1998

This work was supported in part by the Director, Office of Energy Research, Office of Basic Energy Sciences, of the U.S. Department of Energy under Contract No. DE-AC03-76SF00098 and in part by the Air Force Office of Scientific Research, USAF, under grant/contract number FQ8671-96-0-1169.

1. INTRODUCTION

The finite element model TRINET [*Karasaki*, 1987; *Segan and Karasaki*, 1993] calculates transient or steady-state fluid flow and solute transport on a lattice composed of one-dimensional finite elements (i.e., pipes) of porous medium. TRINET incorporates an adaptive gridding algorithm to minimize numerical dispersion for transport calculations. Although TRINET was originally developed to study fracture networks, the primary interest here is in applying TRINET more generally to simulate transport in porous media (or a fractured medium being treated as an effective continuum). This requires developing expressions to relate TRINET inputs to equivalent parameters used to describe flow and transport in homogeneous porous media. In this report, we briefly describe the basic TRINET formulation for flow and transport, present TRINET equivalences for porous medium parameters, and compare TRINET to analytical solutions using the proposed porous medium equivalents.

2. GOVERNING EQUATIONS USED IN TRINET

2.1. FORMULATION FOR FLOW

The flow equation between the two nodes at either end of a one-dimensional finite element may be written as

$$S_s w \frac{\partial h}{\partial t} = T \frac{\partial^2 h}{\partial x^2}, \tag{1}$$

where h is hydraulic head and S_s, w, and T are the specific storage, aperture, and transmissivity, respectively, of the element. The height of each element b is taken to be unity. Hence, the product of specific storage and aperture is storativity: $S_s w = S$. The lattice of elements need not be uniformly spaced: it can be two- or three-dimensional, and rectangular, triangular, or a combination thereof. In the present report, we consider regular rectangular lattices.

Notice that TRINET requires the pair of input parameters (T, S_s), which is somewhat unconventional. Typically, the flow equation is written in terms of the element hydraulic conductivity K and specific storage S_s, where $K \equiv T/w$, or (T, S), where $S = S_s w$. Note that constant head or constant flow boundary conditions can be specified for any node. In this way, wells can be modeled as point sources or sinks located at nodal points, which are the intersections between elements of the lattice.

2.2. FORMULATION FOR TRANSPORT

The transport equation between the two end nodes of a finite element is written as

$$\frac{\partial C}{\partial t} = D^* \frac{\partial^2 C}{\partial x^2} - v_p \frac{\partial C}{\partial x}, \tag{2}$$

where C is the concentration, D^* is the dispersion coefficient of the element and v_p is the pore velocity in the element. Analogous to flow, the concentration boundary conditions may be specified at any node. This is particularly useful if the purpose is to model a contaminant source such as an injection well in a tracer test. In addition, notice that D^* is a direct TRINET input, whereas v_p is not and must be inferred from TRINET concentration breakthrough curves. For the sections pertaining to transport, this discussion is limited to transient solute transport in a steady state flow field only.

3. PROPOSED EQUIVALENCES FOR LATTICES

3.1. PARAMETERS FOR FLOW

3.1.1. 2D FLOW IN A CONFINED AQUIFER

UNIFORM LATTICE SPACING

To simulate flow in a two-dimensional horizontal porous medium, TRINET may be used with a two-dimensional rectangular lattice to represent an areal view of an aquifer. Fig. 1 shows a schematic view of a portion of such a lattice. The distance L gives the lattice spacing, and w and b are the element aperture and height, respectively, for each element in the lattice. The region marked by the dashed line represents the unit cell of the lattice. The following algorithm provides a basis for choosing the element properties S_s, w, and T required for equation (1) so that the lattice as a whole acts like a confined aquifer with storativity $\tilde{S}$ and transmissivity $\tilde{T}$. Although TRINET always uses $b = 1$, treating b as a variable helps make the following derivations clearer.

From Equation (1), it is apparent that the hydraulic conductivity of an element is $K = T/w$, and therefore its conductance (hydraulic conductivity times cross-sectional area) may be written as Kwb. Fig. 1 shows that the conductance through a unit cell of the lattice is exactly this value since the element has hydraulic conductivity K and cross-sectional area wb. The conductance through an equal volume of aquifer would be $\tilde{K}Lb$, where $\tilde{K}$ is the equivalent aquifer hydraulic conductivity. Equating these expressions for conductance gives

$$\tilde{K} = K\frac{w}{L}. \tag{3}$$

Writing this expression in terms of the input variable $T = Kw$ and the desired output variable $\tilde{T} = \tilde{K}b$, and recalling that $b = 1$, give the desired relationship for transmissivity for a lattice with uniform spacing L:

$$\tilde{T} = \frac{T}{L}. \tag{4}$$

The storage of a unit cell of the lattice is given by the element specific storage times the volume of the elements within the unit cell. Since half of four elements (each with length L and cross-sectional area wb) lie within the unit cell, the storage capacity is given by $S_s 2wbL$. The storage

of an equal volume of aquifer would be $\tilde{S}_s bL^2$, where $\tilde{S}_s$ is the equivalent specific storage of the aquifer. Equating these expressions for storage gives

$$\tilde{S}_s = S_s\left(\frac{2w}{L}\right). \tag{5}$$

Writing this expression in terms of the desired output variable $\tilde{S} = \tilde{S}_s b$, and recalling that $b = 1$, give the desired relationship for storativity for a lattice with spacing L:

$$\tilde{S} = S_s\left(\frac{2w}{L}\right). \tag{6}$$

NESTED LATTICE SPACING

For a lattice with variable spacing to behave as a uniform porous medium, element properties must vary with lattice spacing. One example of a lattice with variable spacing is a nested lattice in which a central fine region with spacing L is surrounded by a region with spacing aL, which in turn is surrounded by a region with spacing a^2L, and so on, so that the jth region has lattice spacing a^jL. In Fig. 1 $a = 2$ and portions of the j=0 through j=1 regions are shown. One consistent prescription for lattice element properties is to require that as lattice spacing increases from L to a^jL, the element properties are modified as follows:

$$S_s \rightarrow a^jS_s, \qquad T \rightarrow a^jT, \qquad w \rightarrow w. \tag{7a}$$

Another possible prescription is

$$S_s \rightarrow S_s, \qquad T \rightarrow a^jT, \qquad w \rightarrow a^jw. \tag{7b}$$

These modifications can be easily derived by examining Fig. 1and equating conductance and storage for regions of the lattice with different values of j. Equations (4) and (6) relating effective porous medium properties to lattice properties may be generalized for a nested lattice as follows:

$$\tilde{T} = \frac{T}{a^jL} \qquad \text{and} \qquad \tilde{S} = S_s\frac{2w}{a^jL}. \tag{8}$$

The form of Equation (8) shows explicitly why the prescriptions for T and S given in Equation (7) yield values of $\tilde{T}$ and $\tilde{S}$ that are independent of lattice spacing.

3.1.2. QUASI 3D FLOW IN A LEAKY AQUIFER

UNIFORM LATTICE SPACING

The two-dimensional aquifer model described in the previous section has completely impermeable confining layers above and below it. It is straightforward to extend the model to include small vertical flows into the aquifer through a leaky confining layer. Fig. 2 shows a schematic view of the quasi three-dimensional lattice that is used to accomplish this. One new element and one new

constant-head node are added for each non-boundary node in the original two-dimensional lattice. Each new element has specific storage S_s' , aperture w', transmissivity T', and length L'. Due to the requirement that TRINET elements have height $b = 1$, the cross-sectional area of the new elements is $w'b = w'$, whereas Fig. 2 indicates that it should actually be w'^2. This limitation can be circumvented by using $w' = b = 1$ throughout the lattice.

In order for the confining layer as a whole to have vertical hydraulic conductivity $\tilde{K}'$ and specific storage $\tilde{S}_s'$, vertical conductance and storage for a unit cell of the TRINET lattice are equated to those of a unit cell of the porous medium, as before. For lattice spacing L,

$$K'w'b = \tilde{K}'L^2 \rightarrow \tilde{K}' = \frac{T'}{L^2} \tag{9}$$

$$S_s' bw'L' = \tilde{S}_s' L^2 L' \rightarrow \tilde{S}_s' = S_s'\left(\frac{1}{L^2}\right) \tag{10}$$

where $w' = b = 1$ and $T' = K'w'$ have been used.

NESTED LATTICE SPACING

To account for the variable lattice density, when the lattice spacing increases from L to $a^j L$, the TRINET properties are modified as follows:

$$T' \rightarrow a^{2j}T', \qquad S_s' \rightarrow a^{2j}S_s', \qquad w' \rightarrow w'. \tag{11}$$

At the boundaries between regions of the lattice with different densities, intermediate values of T' and S_s' are used, with a^{2j} in Equation (11) replaced by $0.375\,a^{2j}$ along the edges of the regions, and $0.5625\,a^{2j}$ at the corners. These coefficients are determined by making the conductance and storage as uniform as possible across the density-boundaries in the lattice using unit cell arguments. For the lattice shown in Fig. 3 this correction is not exact, because the different density regions are of very different extents (e.g., the $2\,L = 6$ m region of the lattice is only one element wide, while the $4\,L = 12$ m region is eight elements wide). For a lattice with continuously increasing density (each region of the lattice is only one element wide), the appropriate correction factors would be $0.333\,a^{2j}$ for edges and $0.2857\,a^{2j}$ for corners. Equations (9) and (10) can be generalized for a nested lattice as follows:

$$\tilde{K}' = \frac{T'}{(a^j L)^2} \tag{12}$$

$$\tilde{S}_s' = \left(\frac{S_s' w'}{(a^j L)^2}\right). \tag{13}$$

3.2. PARAMETERS FOR TRANSPORT

For simulating transport in a steady-state flow field, algorithms are developed for choosing element properties required for equation (2) so that a TRINET lattice behaves as a homogeneous porous medium with hydraulic conductivity $\tilde{K}$, hydrodynamic dispersion $\tilde{D}$, and effective porosity ϕ. Four types of transport problems are considered: longitudinal transport through a 1D pipe, longitudinal transport in a 2D porous medium, longitudinal tranport in a 3D porous medium, and transport in a radially divergent flow field. In all four problems, it is assumed that solute is released in a steady state flow field and the solute concentration at the source, C_0, is held constant. Although the effective porosity ϕ does not appear explicitly in equation (2), it is required because the rate at which solute is transported through the medium is

$$v_p = \frac{v_d}{\phi} \tag{14}$$

where the Darcy velocity v_d is given by the ratio of specific discharge to the cross-sectional area normal to flow:

$$v_d = \frac{Q}{A}. \tag{15}$$

For a given aquifer with parameters $\tilde{K}$, $\tilde{D}$ and ϕ, an equivalent set of TRINET input parameters is determined so that TRINET accurately simulates transport through the aquifer using a lattice. Note that the set of equivalent TRINET parameters depends on lattice dimension and the orientation of lattice elements to the flow field. These equivalence expressions are verified by comparison to either an analytical solution or an approximation to an analytical solution. For the case of the 3D medium, an algorithm is presented, but not verified.

3.2.1. 1D TRANSPORT IN A 1D MESH

A pipe of length L_p, width w_p, and thickness b_p is filled with fluid. The hydraulic conductivity through the pipe is $\tilde{K}$. In TRINET, a one-dimensional input mesh can be used to simulate 1D transport through the pipe. The one-dimensional input mesh is simply a series of nodes connected along a line by elements of equal lengths L with S_s, w, b, D, and T denoting the specific storage, aperture, thickness, dispersion coefficient, and transmissivity, respectively, of each element. A schematic diagram of a mesh for a 10 m pipe is shown for example in Fig. 4. Alternatively, the mesh could consist of a single element of length L_p. To assign element transmissivity, recall from Section 2.1 that an element with transmissivity T has hydraulic conductivity $K = T/w$. Hence the conductance in the TRINET pipe element is Kwb. A pipe with hydraulic conductivity $\tilde{K}$ has conductance $\tilde{K}w_p b_p$. Equating conductances implies T should be chosen to satisfy

$$T = \frac{\tilde{K} w_p b_p}{b}. \tag{16}$$

For a 1 m thick pipe, TRINET can simulate transport only when the effective porosity of the medium is $\phi = 1$. This is obvious by observing that the effective volume available for transport in the pipe is the product of the pipe volume and the effective porosity, which is $\phi w_p b_p L_p$. If $\phi = 1$, this is exactly the effective volume transport in the fracture element since $w = w_p$ and $b = b_p = 1$. This is obvious since the pipe and the 1D mesh have the same volume and TRINET assumes a fracture element consists entirely of void space.

In addition, if the element dispersion coefficient is set equal to the value of the dispersion coefficient of the pipe and steady-state flow through the pipe is assumed, then the TRINET element parameter values required to simulate transport through the pipe in addition to (16) are

$$\tilde{D} = D \qquad \phi = 1 \tag{17}$$

for $w = w_p$ and $b = 1$.

3.2.2. 2D LATTICE WITH UNIFORM SPACING

In this section an equivalent set of TRINET input parameters is developed for longitudinal transport through an aquifer with dispersion coefficient $\tilde{D}$ and effective porosity ϕ when transport is simulated on a 2D lattice. A 10 m by 10 m uniform lattice is shown for example in Fig. 5. Here, the lattice represents a rectangular slab of a porous medium with length L_p, width w_p, and thickness $b_p = b = 1\text{m}$. A solute with concentration $C_0 = 1.0$ is released on the left hand side and is transported across the slab by advection and dispersion. The hydraulic conductivity, storativity, and porosity of the medium are denoted by $\tilde{K}$, $\tilde{S}$, and ϕ respectively. The dispersion through the slab is denoted by $\tilde{D}$. Each lattice element has a transmissivity T, aperture w, length L, thickness b, specific storage S_s, and dispersion coefficient D. To develop an algorithm for dispersion, we first recognize that the flow equation and the diffusion equation have the same mathematical form with the hydraulic diffusivity, $\tilde{\alpha}$, playing a similar role in the flow equation to the dispersion coefficient, $\tilde{D}$, in the diffusion equation. We will take advantage of this similarity by deriving an expression for hydraulic diffusivity and propose an analogous equivalence for the dispersion coefficient. Recall that the one dimensional flow equation rewritten in terms of $\tilde{\alpha}$, the hydraulic diffusivity, is

$$\frac{\partial h}{\partial t} = \frac{\tilde{K}}{\tilde{S}_s}\frac{\partial^2 h}{\partial x^2} = \tilde{\alpha}\frac{\partial^2 h}{\partial x^2}. \tag{18}$$

Equation (18) is of the same mathematical form as the one-dimensional diffusion equation,

$$\frac{\partial C}{\partial t} = \tilde{D}\frac{\partial^2 C}{\partial x^2}. \tag{19}$$

This similarity suggests that arguments for $\tilde{\alpha}$ for the flow problem can be applied analogously to $\tilde{D}$ for the transport problem. Since

$$\tilde{\alpha} \equiv \frac{\tilde{K}}{\tilde{S}_s}, \tag{20}$$

the hydraulic diffusivity can be written in terms of the TRINET element diffusivity, $\alpha = K/S_s$ as

$$\tilde{\alpha} = \frac{\tilde{K}}{\tilde{S}_s} = \frac{Kw / L}{S_s 2w / L} = \frac{\alpha}{2} \tag{21}$$

by using equations (3) and (5).This suggests the equivalence

$$\tilde{D} = \frac{D}{2}. \tag{22}$$

This implies that dispersion in an aquifer with a dispersion coefficient $\tilde{D}$ can be simulated by TRINET if the element dispersion coefficient is chosen to be twice the value of the aquifer dispersion coefficient.

In order to develop an algorithm for determining the correct element parameter values so that a two-dimensional lattice behaves like a porous medium with effective porosity ϕ, two uniform lattices are considered: a "linear" lattice (Fig. 5), and a "diagonal" lattice (Fig. 6). The flow direction is horizontal and parallel to the x-direction. The lattices differ in orientation and overall size, however, a $L = 1$ m lattice spacing is used for both. In the linear mesh, elements are either parallel or perpendicular to the direction of flow, and in the diagonal mesh, all elements are at a 45 degree angle to the flow direction.

Consider a $L \times L$ m unit cell in the linear mesh. Fig. 7 shows a section of the lattice and the boundaries of a unit cell (shaded gray). The effective porosity of the lattice is given by the ratio V_1/V_2, where V_1 is the volume of lattice space available for transport (effective volume of pore space) in the unit cell and V_2 is the volume of the unit cell. Since the lattice represents a slab with uniform thickness b, $V_2 = bL^2$. The volume of lattice space used for transport in TRINET is the volume contribution of the two element halves along the flow direction so $V_1 = 2(wb\ L/2)$. If the lattice is to represent a porous medium with effective porosity ϕ, then the aperture must be chosen to satisfy

$$\phi = \frac{V_1}{V_2} = \frac{2(wb\ L/2)}{bL^2} = \frac{wb}{Lb} = \frac{w}{L}. \tag{23}$$

Note that only two of the four half-elements are counted since there is no tranport per se in the elements perpendicular to flow. In TRINET these elements can be filled by the solute due to dispersion, but once these elements are occupied, no more solute can enter. Hence, these elements essentially do not participate in the advective part of solute transport and are not counted in the pore volume.

For the diagonal mesh, all finite elements are used in transport. Consider the unit cell as shown in Fig. 8. The diagonal lattice has $L = 1$ m spacing so the dimensions of the unit cell are $\sqrt{2}L \times \sqrt{2}L \times b$ m. The cell volume is $V_2 = b(\sqrt{2}L)^2 = 2bL^2$, and the effective volume of pore space is the total volume of the four intersecting elements so that $V_1 = 4bwL$. If the

diagonal lattice is to behave as a porous medium with an effective porosity ϕ, the aperture must be assigned a value so that

$$\phi = \frac{V_1}{V_2} = \frac{4bwL}{2bL^2} = \frac{2w}{L}. \tag{24}$$

Therefore, the TRINET element parameters in the linear lattice must be chosen to satisfy

$$\tilde{D} = \frac{D}{2} \qquad \phi = \frac{w}{L} \tag{25}$$

as given by (22) and (23). In the diagonal lattice, the TRINET element parameters must be chosen to satisfy

$$\tilde{D} = \frac{D}{2} \qquad \phi = \frac{2w}{L}. \tag{26}$$

as given by (22) and (24). This means that for an aquifer with dispersion coefficient $\tilde{D}$ = 1.0e-04 m^2/s and effective porosity ϕ = 0.3, a 2D lattice with 1 m length elements should have the element dispersion coefficient set to D = 2.0e-04 m^2/s for both the linear lattice and the diagonal lattice. In the linear lattice, the aperture should be set to w = 0.3 m. The apertures in the diagonal lattice must be half as large as the apertures in the linear lattice (w = 0.15 m).

3.2.3. 3D LATTICE WITH UNIFORM SPACING

In this section, an equivalent set of TRINET parameter values are developed for $\tilde{D}$ and ϕ for simulating longitudinal transport in a 3D lattice (i.e., the elements are either parallel or perpendicular to the flow direction). Here, the lattice represents a volume of porous medium with length L_p, width w_p, and thickness b_p. The hydraulic conductivity, storativity, effective porosity, and dispersion of the medium are denoted by $\tilde{K}$, $\tilde{S}$, ϕ, and $\tilde{D}$ repectively. For a uniform 3D lattice of elements with transmissivity T, aperture w, specific storage S, length L, thickness b, and dispersion coefficient D, the relationship between D and $\tilde{D}$ can be derived by analogy to the relationship for hydraulic diffusivity. Note that L is chosen so that $L>>b$ and $L>>w$ so that each element represents a rod-shaped rectangular solid with volume wbL.

The conductance through the lattice is given by $nKwb$ ($K = T/w$) where n is the number of elements on the left face that contribute to the cross-sectional area perpendicular to the direction of flow. Since the lattice has uniform spacing, $n = b_p/L \times w_p/L$. The conductance through the equivalent porous medium is given by $\tilde{K}w_p b_p$. Equating these conductances yields

$$\tilde{K} = \frac{T/w\ wb}{w_p b_p}\left(\frac{b_p w_p}{L^2}\right) = \frac{Tb}{L^2}. \tag{27}$$

Note that this coincides with equation (9) when the element thickness b is unity.

Now consider the unit cell shown in Fig. 9. The unit cell is a cube with sides of length L and centered about a lattice node. Since each of the six half-elements contributes a volume of $wb\ L/2$, the storage in the unit cell is given by $S = 6S_s wb\ L/2$. For the equivalent porous medium, the storativity is given by $\tilde{S} = \tilde{S}_s L^3$. Equating these quantities yields

$$\tilde{S}_s = \frac{6S_s wb\ L/2}{L^3} = 3S_s\ wb/L^2 . \tag{28}$$

Flow through the lattice can be modeled by TRINET if T, S_s, and w are chosen to satisfy $\tilde{K} = Tb/L^2$ and $\tilde{S}_s = 3S_s(wb/L^2)$. Hence the effective hydraulic diffusivity is

$$\tilde{\alpha} = \frac{\tilde{K}}{\tilde{S}_s} = \frac{Tb/L^2}{3S_s(wb/L^2)} = \frac{T}{3wS_s} = \frac{K}{3S_s} = \frac{\alpha}{3}, \tag{29}$$

which implies that the 3D lattice behaves as a porous medium with dispersion $\tilde{D}$ if D is chosen to satisfy $\tilde{D} = D/3$. The equivalence for the porosity is obtained by referring to the unit cell in Fig. 9. The volume of the unit cell is $V_2 = L^3$. If the flow is horizontal (as indicated in Fig. 9), the volume of lattice space in the unit cell is the total volume contribution of the two half-elements parallel to the flow. The four remaining half-elements are perpendicular to the flow direction so no advection occurs along these elements. Since each element has length L, width w, and thickness b, $V_1 = 2wb\ L/2$. In order that the fraction of pore volume match the aquifer porosity, w should be chosen to satisfy

$$\phi = \frac{V_1}{V_2} = \frac{2wb\ L/2}{L^3} = \frac{wb}{L^2} . \tag{30}$$

Note that setting $b = w$ simplifies this expression to $\phi = w^2/L^2$.
By analogy with the 2D case (Section 3.2.2), we assume that for diagonal flow, which occurs parallel to one plane of the lattice, but not parallel to any of the elements within that plane, w should be chosen so that $\phi = 2wb/L$. For flow that is not aligned with any lattice plane, all elements will be used in transport and w should be chosen so that $\phi = 3wb/L^2$.

3.2.4. NESTED LATTICES

In this report, nested lattices are not considered for modelling transport. Typically, the application for nested lattices is in simulating flow (such as in a confined aquifer) where the mesh boundary must extend far beyond the well field so that with the prescribed boundary conditions, the mesh behaves as an infintely extending medium. Since resolution is required in the vicinity of the well field but not necessarily near the boundary, the nested lattice is an economical compromise between the need for resolution and the computation burden of a uniformly fine mesh. The situation is not the same for simulating transport for several reasons. In field experiments, tracer tests are usually conducted under steady-state flow conditions, so that modelling tracer transport does not require a mesh with extended boundaries (as is the case with modelling well test data and matching pressure transients). If resolution greater than that offered by the uniform lattice is required, the obvious choice is not the nested lattice. On the contrary, in the radial transport problems described in Sections 4.4 and 4.5, pore velocity decreases with radial distance so resolution is required in the outer region of the mesh, not near the center. In this case, a mesh with increasingly finer regions away from the contaminant source (e.g., the mesh center) is preferable. Beyond the applicability of nested lattices, there are difficulties in constructing such a mesh as well as computational issues. For example, if a lattice with a coarse center and fine outer region is input to TRINET, the mesh could easily be large enough (based on the number of nodes) that memory requirements and run time would make using TRINET impractical. For example, doubling the number of nodes can result in a four-fold increase in run time. In addition, the number of additional advective or

dispersive nodes that must be added in order to accurately model transport in the coarse region might also be unreasonably large. This would occur in the event of a sharp concentration gradient or if the velocity in elements is low.

4. APPLICATION AND COMPARISON TO ANALYTICAL SOLUTIONS

4.1. COMPARISON TO THEIS SOLUTION FOR 2D TRANSIENT FLOW

The ability of TRINET to properly model flow through a porous medium has been verified by comparing its results to the Theis solution for transient radial flow in a confined homogeneous isotropic aquifer, in which a fully-penetrating well is pumped at a constant flow rate [*Theis*, 1935]. The lattice used for the calculation (see Fig. 3) was developed to model an aquifer with a well-field shown by the solid circles, with the pumping well at the center (x=0, y=0). The spacing in the central region of the lattice is $L = 3\text{m}$, and the aperture throughout the lattice is $w = 1\text{m}$. The nested lattice design is practical for modeling flow in porous media, where fine resolution is needed to represent flow near well adequately, but the lattice must extend far beyond the well field to realistically implement pressure boundary conditions. Fine resolution is undesirable beyond the well field because it greatly increases the size of the calculation without improving the ability of the model to predict flow or pressure at the well field.

Fig. 10a compares the Theis solution to the dimensionless drawdown calculated by TRINET using the material properties and boundary conditions shown in Table 1. Overall, the match is excellent. The open circles in Fig. 3 show the locations where the drawdowns are compared. An equally good match is obtained if the drawdowns are compared along a line parallel to the x- or y-axis. The calculation was also done with a finer nested lattice in which $L = 3\text{m}$ throughout the region defined by -120 m < x < 120 m and -120 m < y < 120 m, beyond which lattice spacing was successively doubled. A comparison of the calculated drawdowns to the Theis solution is shown in Fig. 10b. Although the match is even better than in Fig. 10a the fine lattice contains about 9,000 nodes and 17,000 elements as compared to 800 nodes and 1,500 elements for the lattice shown in Fig. 3. Computer time roughly increases by a factor $2m$ when the number of nodes and elements increases by a factor m. If TRINET is implemented as part of an inversion in which many forward calculations must be made, the nested lattice in Fig. 3 is preferable to the fine mesh since it provides a good compromise between accuracy and efficiency.

Table 1. Parameters for Theis solution verification.

TRINET Input Parameters	Equivalent Porous Medium Properties
Material Properties and System Dimensions	
T = 3.0e-03 m^2/s †	$\tilde{T}=\frac{T}{L}$ = 1.0e-03 m^2/s
S_s =5.6e-05 m^{-1} †	$\tilde{S}=S_s\frac{2w}{L}$ = 3.73e-05 m^{-1}
b = 1 m	b = 1 m
Initial and Boundary Conditions	
h = 0 for all x and y at t =0	h =0 for all r at t =0
h = 0 at x=y=± 600 m ‡	h = 0 as $r \rightarrow \infty$
Q =0.333e-03 m^3/s at x=y=0	Q =0.333e-03 m^3/s at r =0

† Used in the finest region of the lattice, where L = 3m; where lattice spacing is $a^j L$, $T \rightarrow a^j T$ and $S_s \rightarrow a^j S_s$.

‡ Calculation time is short enough so that a finite lattice acts like an infinite medium.

4.2. COMPARISON TO HANTUSH & JACOB SOLUTION FOR QUASI 3D TRANSIENT FLOW

Fig. 11a compares the results of TRINET using the quasi three-dimensional nested lattice described in Section 3.1.2 to an analytical solution for transient radial flow in a homogeneous isotropic aquifer with a slightly leaky confining layer, in which a fully-penetrating well is pumped at a constant flow rate [*Hantush and Jacob*, 1955]. In the confining layer, flow is taken to be purely vertical, storage is assumed to be negligible, and head is held fixed, making the leakage into the aquifer act like a source term proportional to aquifer drawdown. Tables 1 and 2summarize the material properties and boundary conditions used. The parameter B, which is used to scale radial distance from the pumping well, is given by $B = \left(\tilde{K}bb'/\tilde{K}'\right)^{1/2}$ = 170m [*Doughty*, 1995]. The TRINET drawdowns for the locations marked by the open circles in Fig. 3 reproduce the analytical solution quite well, especially for the values of $r/B \leq 1.0$. Use of the alternate edge and corner correction factors described in Section 3.1.2 improves the match for large values of r/B at the expense of the smaller ones, which is undesirable for the intended purpose of this lattice to model the drawdown at the wells shown as solid circles in Fig. 3. The calculation was repeated using the finer nested lattice described above, and Fig. 11b shows that a better match to the analytical solution can be obtained. As in the case of the two-dimensional lattice, the increased computation time for the fine lattice makes its use impractical in an inverse method, and the accuracy of the lattice shown in Fig. 3 provides an adequate representation of a slightly leaky aquifer.

Table 2. Parameters for *Hantush and Jacob* [1955] solution verification, in addition to those given in Table 1.

TRINET Input Parameters	Equivalent Porous Medium Properties
Confining Layer Properties and Dimensions	
$T' = 1.9\text{e-}06\ \text{m}^2/\text{s}$ †	$\tilde{K}' = \frac{T'}{L^2} = 2.11\text{e-}07$ m/s
$S_s' = 5.6\text{e-}13\ \text{m}^{-1}$ †‡	$\tilde{S}' = S_s' \frac{w}{L^2} = 6.22\text{e-}14\ \text{m}^{-1}$ ‡
$b' = 6.1$ m	$b' = 6.1$ m
Boundary Condition in Confining Layer	
$h = 0$ for all x and y at $z = b'$	$h = 0$ for all r at $z = b'$

† Used in the finest region of the lattice, where $L = 3$m; where lattice spacing is $a^j L$, $T' \rightarrow a^{2j} T'$ and $S_s' \rightarrow a^{2j} S_s'$.

‡ $\tilde{S}_s'$ is assumed to be zero in the analytical solution.

4.3. ONE-DIMENSIONAL TRANSPORT

In the 1D transport problem, a slab of length L_p, width w_p, and thickness b_p is filled with a porous medium of porosity ϕ. The hydraulic conductivity and storage of the medium are $\tilde{K}$ and $\tilde{S}$, respectively, and the longitudinal dispersion in the slab is $\tilde{D}$. The pressure is held fixed at the ends of the slab:

$$h(0, t) = h_1 \quad t > 0$$
$$h(L_p, t) = h_2 \quad t > 0$$

with $h_1 > h_2$. Applying Darcy's law to determine the steady-state flow rate, the discharge is

$$Q = -\tilde{K}A\left(h_2 - h_1\right)/L_p,$$

which implies a Darcy velocity of $v_d = Q/A = -\tilde{K}\left(h_2 - h_1\right)/L_p$. A source is located at $x = 0$m with concentration $C_0 = 1.0$. The solute is transported by advection and dispersion under steady-state flow. The one-dimensional advection dispersion equation is

$$\tilde{D}\frac{\partial^2 C}{\partial x^2} - v_p \frac{\partial C}{\partial x} = \frac{\partial C}{\partial t},$$

where C is the solute concentration. The concentration at a distance x along the pipe at time t with initial concentration C_0 is given by the analytical solution [*Ogata and Banks,* 1961]

$$C(x,t) = \frac{C_0}{2}\left[\operatorname{erfc}\left(\frac{x - v_p t}{\sqrt{4\tilde{D}t}}\right) + \exp\left(\frac{v_p x}{\tilde{D}}\right)\operatorname{erfc}\left(\frac{x + v_p t}{\sqrt{4\tilde{D}t}}\right)\right]. \tag{31}$$

Since C_0=1.0, the concentrations calculated by TRINET are referred to as relative concentrations.

In Sections 4.3.1, 4.3.2, and 4.3.3 below, the relations derived in sections 3.2.1 and 3.2.2 are verified in two steps. First, expressions for $\tilde{D}$ are verified by simulating transport with TRINET when the hydraulic gradient is set to zero. TRINET breakthrough curves are plotted together with breakthrough curves from the analytical solution substituting the value for $\tilde{D}$ prescribed by equation (17) or (25) or (26). Agreement between the breakthrough curves is verified by inspection. Second, expressions for the porosity are verified by simulating advection only. In TRINET, the element dispersion coefficient is expected to be nonzero so the dispersion parameter is set to a very small value so that dispersion can be considered negligible. The TRINET breakthrough curves are plotted and the pore velocity is estimated at several time steps. Since the estimated pore velocities are expected to vary at each time step, an average is taken for the overall estimated pore velocity. $\tilde{D}$ is set to zero and the estimated pore velocity is substituted for the pore velocity in the analytical solution. The breakthrough curves from the analytical solution are compared with the TRINET breakthrough curves and agreement is verified by inspection. Next, given the values of T, w, and L specified in the lattice, the equivalent porosity and dispersion prescribed by (17) or (25) or (26) are calculated, and it is demonstrated that the estimated pore velocity agrees with the velocity predicted via equation (14) and (17) or (25) or (26). The method for estimating the pore velocity is described in section 4.3.1.

4.3.1. 1D MESH

In TRINET, transport is simulated in a pipe of length L_p = 10m with the mesh shown in Fig. 4. The mesh consists of ten 1m elements with the same element parameter values for transmissivity T, aperture w, specific storage S_s, and dispersion D. Each element has thickness b = 1 m. Here, T = 5e-08 m^2/s, w = 5e-05 m, S_s = 1e-05 m^{-1}, and D = 1e-09 m^2/s. The pressure is held fixed at the ends of the mesh at h_1 = 10 m and h_2 = 0.0 m.

With the TRINET inputs above, the TRINET Darcy velocity is

$$\begin{aligned} v_d &= \frac{Q}{A} \\ &= -K\,\nabla h = \frac{-T\nabla h}{w} = 1.0\text{e-}03 \ \text{m/s} \end{aligned} \tag{32}$$

To compare the TRINET solution to the analytical solution, the algorithms for $\tilde{D}$ and ϕ from section 3.2.1 are checked by applying the two-part procedure described in Section 4.3. First, $\tilde{D}$ is inferred by comparing TRINET breakthrough curves to the analytical solution breakthrough curves when there is no advection (i.e., diffusion only). This is easily achieved in TRINET by imposing a zero hydraulic gradient (i.e., setting $h_1 = h_2$ = 0.0 m). By trial and error the best match is obtained when the element dispersion coefficient is identical to the aquifer dispersion coefficient ($D = \tilde{D}$). The pore velocity, v_p, is then inferred by analyzing breakthrough curves

when dispersion is minimal. Since pore velocities are not directly output by TRINET, the velocity is estimated as follows. A breakthrough is recorded at the first position x_5 and time t where the relative concentration $C(x_5, t) = 0.5$. In some cases, this location is obtained by linear interpolation. The pore velocity is then estimated by $v_{p_{est}} = x_5/t$. Breakthrough curves are calculated independently via the analytical solution in equation (31) inputting the values for $\tilde{D}$ and v_p prescribed by equations (14) and (17). TRINET breakthrough curves are plotted together with the analytical solution curves to verify that the breakthroughs match. Figs. 12 and 13 show the TRINET simulation and the analytical solution under pure diffusion (i) and pure advection (ii). D = 2.0e-04 m^2/s to correspond to $\tilde{D}$ = 1.0e-04 m^2/s in the diffusion-only case. In the advection-only case, D = 1.0e-09 m^2/s to correspond to $\tilde{D}$ 5.0e-10 m^2/s in order to set the dispersion essentially to zero. The TRINET solution is indicated by the plotting symbols and the analytical solution is indicated by the solid line. Overall, the agreement between TRINET and the analytical solution is excellent.

From the TRINET breakthrough curves in Fig. 13, the pore velocity was estimated to be 1.00e-03 m/s. In addition, when the TRINET element transmissivities, apertures, and specific storages are perturbed, and the resulting pore velocities are estimated, we find that

$$\begin{aligned} v_{p_{est}} &\propto T \\ &\propto 1/w \\ &\propto \Delta h \end{aligned}$$

In addition, we find that the estimated pore velocity coincides with the Darcy velocity. In other words,

$$v_{p_{est}} \cong \frac{T\ \nabla h}{w}.$$

This implies that the TRINET effective porosity for this mesh is $\phi = 1$, which is in agreement with equation (17). As expected, the pore velocity does not depend on element length (i.e., the discretization). For verification, this experiment was repeated for a 1D mesh with twenty 0.5m elements, and the pore velocity was estimated to be 1.18e-03 m/s, which compares quite well to the expected pore velocity.

4.3.2. 2D LINEAR MESH

Here, the 2D uniform lattice described in section 3.2.2 is used to simulate 1D transport. Now the mesh represents a thick slab of some material with porosity $\phi < 1$ since tracer is allowed to travel only along the bonds of the lattice. The "linear" mesh used for TRINET is shown in Fig. 5. The element inputs for this case are: T = 5e-08 m^2/s, w = 5e-05 m, S_s = 1e-05 m^{-1}, D = 1e-09 m^2/s and L = 1 m. Inferring $\tilde{D}$ under a zero hydraulic gradient leads to $\tilde{D} = D/2$, which verifies the proposed TRINET equivalent for dispersion (equation (22)). Inferring the TRINET pore velocity with a very small amount of dispersion (nearly pure advection) leads to observing that

$$
\begin{aligned}
v_{p_{est}} &\propto T \\
&\propto 1/w \\
&\propto \nabla h
\end{aligned}
$$

and

$$
v_{p_{est}} \cong \frac{T\,\nabla h}{w}.
$$

The simulated breakthrough curves agree extremely well with the analytical solutions for the advection only case (Fig. 14) and the diffusion only case (Fig. 15). Note that the accuracy of pore velocity estimates improves substantially with a finer mesh (0.5 m spacing) and when the time step incrementing parameter prr is reduced from 1.4 to 1.1. See *Segan and Karasaki* [1993] for details on prr. The Darcy velocity for this rectangular 2D mesh is (Equation (3)):

$$
v_d = -\tilde{K}\,\nabla h = \frac{T}{L}\,\nabla h.
$$

Thus porosity is given by $\phi = v_d/v_p = w/L$, which verifies the expression for porosity in equation (25).

4.3.3. 2D DIAGONAL MESH

For the diagonal lattice in Fig. 6, a larger porosity is expected since all of the elements are used in simulating transport. In fact, for the diagonal mesh, we expect the porosity to be twice as large as the linear 2D mesh since the solute can travel along a path that makes use of all the elements instead of only those in the x-direction (half of the elements in the 2D linear mesh). The element inputs for the 2D diagonal mesh are T = 5e-08 m^2/s, w = 5e-05 m, S_s = 1e-05 m^{-1}, L = 1.0 m, b = 1.0 m, and D = 1e-09 m^2/s.

Inferring D by comparing concentrations under pure diffusion gives an excellent match when $\tilde{D} = D/2$ is used in the analytical solution (Fig. 16). Simulating transport under pure advection, and doubling and halving values of TRINET element inputs, the pore velocity is estimated to be close to 5.0e-04 m/s and

$$
\begin{aligned}
v_{p_{est}} &\propto T \\
&\propto 1/w \\
&\propto \nabla h \\
v_{p_{est}} &\cong \frac{1}{2}\,\frac{T\,\nabla h}{w}.
\end{aligned}
$$

Thus porosity is given by $\phi = v_d/v_p = 2w/L$, which is in agreement with the porosity predicted by equation (26). For the advection only case, TRINET also matches the analytical solution. Fig. 17 gives the TRINET breakthrough curves at several times and the analytical solution plotted for comparison.

4.4. TRANSPORT IN A RADIALLY DIVERGENT FLOW FIELD WITH CONSTANT DISPERSION

In this section we compare TRINET to an analytical solution for the problem of transport in a radially divergent flow field (steady state flow). In this problem, contaminant is released from a well of radius $r_w = a$ (meters) and the contaminant is transported radially by advection and dispersion. The aquifer is a homogeneous, isotropic, confined aquifer with thickness $b = 1$ m. The aquifer has transmissivity $\tilde{T}$ and effective porosity ϕ, and the rate of release (volumetric flow rate) and concentration at the injection well are constant. The governing equation for advective heat transport is given by *Carslaw and Jaeger* [1946]. The analogous solution for mass transport is

$$\tilde{D}\left(\frac{\partial^2 C}{\partial r^2} + \frac{1}{r}\frac{\partial C}{\partial r}\right) - v_p \frac{\partial C}{\partial r} = \frac{\partial C}{\partial t}, \tag{33}$$

where r is radial distance, v_p is the radial velocity, and $\tilde{D}$ is the lumped dispersion coefficient. The pore velocity is given by

$$v_p = \frac{Q}{2\pi\, r\phi b}, \tag{34}$$

where Q is the volumetric flow rate at the well. Note that the pore velocity is positive for a divergent flow field and negtative for a convergent flow field. Under the conditions

$$\begin{aligned} C(r, t = 0) &= 0.0 \text{ for all } r > a && \text{(initial condition)} \\ C(a, t) &= 1.0 \text{ for all } t \geq 0 && \text{(boundary condition)} \\ C(r = \infty, t) &= 0.0 \text{ for all } t \geq 0 && \text{(boundary condition)} \end{aligned}$$

and steady-state flow, the analytical solution given by *Carslaw and Jaeger* [1946] is

$$C(r,t) = C_0 + \frac{2C_0}{\pi}\left(\frac{r}{a}\right)^k \int_0^\infty \frac{e^{-\tilde{D}u^2 t}\left[J_k(ur)\,Y_k(ua) - Y_k(ur)\,J_k(ua)\right]}{u\left[J_k^2(ua) + Y_k^2(ua)\right]}\,du, \tag{35}$$

where J_k and Y_k are k^{th} order Bessel functions and $k = q/(4\pi\,\tilde{D})$.

4.4.1. EQUIVALENT PARAMETERS FOR RADIAL TRANSPORT PROBLEM

UNIFORM 2D LATTICE

The TRINET lattice shown in Fig. 18 is generated to simulate transport. Based on the set of equivalent TRINET input parameters developed for the 1D transport problem (section 3.2.2), it is reasonable to choose values for element parameters D and w for the transport problem that satisfy

$$\tilde{D} = D / 2 \qquad \text{and} \qquad \phi = \frac{2w}{L}.$$

The effective porosity $\phi = 2w/L$ is used since TRINET simulates transport using most of the elements in the lattice when the flow field is radial.

Note that the radial mesh is "trimmed" to a 20 m radius. Trimming is done in order to reduce the number of nodes and hence ease computational efforts and to apply the correct outer boundary conditions for flow and transport. The transmissivity is $\tilde{T}$ = 5.0e-08 m^2/s and the well radius is $r_w = a = 1$ m. A well with a 1 m radius is modeled by the four nodes marked by filled diamonds at the center of the lattice (Fig. 18). The four nodes are required in order to accurately simulate a radial flow field in TRINET. A simple procedure is used to determine the appropriate injection rate at each well node so that a unit hydraulic head gradient is simulated between the well center and the lattice boundary. It is determined that a flow rate at each well node of 5.24e-07 m^3/s is appropriate. The total flow rate is Q_{TRINET} = 2.1e-06 m^3/s. Details of this procedure are described in Appendix 1.

Due to boundary effects, a larger mesh was required so a mesh with a 40 m radius was constructed. Unfortunately, the number of nodes for this mesh is quite large and due to computational constraints, only a quarter of the mesh is considered (Fig. 19). The TRINET solution is unaffected due to the symmetry of the lattice. Note that there are now only two injection wells, each with half of their original flow rate or $Q_{node} = \frac{1}{8} Q_{TRINET}$ =2.62e-07 m^3/s.

4.4.2. NUMERICAL EVALUATION OF THE ANALYTICAL SOLUTION (SCIENTIST PROGRAM)

In order to compare the TRINET simulation to the analytical solution, a program was written to numerically integrate the solution in equation (35). The program uses a commercial integration package (Scientist program). The analytical solution is evaluated at radial distance r, and time t, with input parameters $\tilde{D}$ for dispersion, well radius a (fixed at a = 1 m), and a volumetric flow rate Q_{sci} as input for the velocity. The flow rate Q_{sci} is the total flow rate at the well radius. The pore velocity at radius r is actually given by

$$v_p = Q_{sci} \; / \; (2\pi r b) .$$

Note that the analytical solution assumes a unit effective porosity so that the pore velocity in the analytical solution coincides with the Darcy velocity. In order for TRINET to produce breakthrough curves with the same pore velocity, the flow rate must be adjusted by the effective porosity of the lattice. The appropriate flow rate input to the Scientist program is

$Q_{sci} = \dfrac{Q_{TRINET}}{2w \; / \; L}$. For the TRINET inputs specified, this gives

$$Q_{sci} = \frac{2.0974\text{e}{-06}\ \text{m}^3/\text{s}}{(2 \times 5\text{e}{-05}\ \text{m}/1\text{m})} \cong 2.1\text{e}{-02}\ \text{m}^3/\text{s} .$$

4.4.3. COMPARISON TO ANALYTICAL SOLUTION

In order to verify that the equivalence for dispersion in equation (26) also holds for radial transport, we follow the procedure described in Section 4.3.1 for estimating TRINET pore velocities from breakthrough curves. TRINET breakthrough curves simulating diffusion only are compared to breakthrough curves calculated by the Scientist program. In addition, TRINET and the Scientist program are checked by comparison to a solution for the diffusion only problem

published by *Jaeger* [1956]. Concentrations at specific times for several radial distances under pure diffusion are compared. Fig. 20 shows an excellent match between the TRINET simulation, the Scientist program, and the solution by *Jaeger* [1956]. The open circles indicate concentrations calculated by TRINET at nodes located along a 45 degree angle. The open triangles indicate concentrations calculated by TRINET at nodes located along the horizontal.

Based on the results in section 4.3.3, the TRINET equivalent for radial velocity is expected to be close to

$$v_p(r,\,t) \cong \frac{v_{darcy}(r,\,t)}{2w/L} = \frac{Q_{TRINET}/(2\pi\, r(t)\, b)}{2\, w\, /L}.$$

The expression for pore velocity was verified by comparison with the analytical solution for two values of $\tilde{D}$. Figs. 21 and 22 show the location of the front at three times for a case with moderate dispersion ($\tilde{D}$ = 5e-04 m^2/s) and a case with a small amount of dispersion ($\tilde{D}$ = 5e-05 m^2/s). For the case with moderate dispersion (Figs. 21a – 21c), the agreement is very good for nodes located along the 45 degree line (along the diagonal). As expected, the front appears to move faster along the x-direction than along the diagonal. Again, this is an effect due to the mesh since the flow path in the x-direction is shorter on average, because elements perpendicular to the flow direction do not participate in advective transport.

When the dispersion is small (Figs. 22a – 22c), the agreement is not as good. Although the contrast in $\tilde{D}$ is only one order of magnitude, difficulties arise in calculating values from the analytical solution. This appears to be the smallest value of dispersion that can be input before the Scientist program shows signs of numerical instability. In addition, there are problems selecting stable parameter values for integration. The Scientist program appears to be sensitive to integration limits and step size, particularly for smaller values of dispersion. This makes the Scientist program cumbersome to use because of the need to constantly "fine tune" integration limits. Fortunately, TRINET concentrations are easily obtained in this case and for dispersion values as small as $\tilde{D}$ = 5e-06 m^2/s (i.e., D = 1e-05 m^2/s).

4.5. TRANSPORT IN A RADIALLY DIVERGENT FLOW FIELD WITH CONSTANT DISPERSIVITY

In equation (33) the hydrodynamic dispersion $\tilde{D}$ was assumed to be a constant lumped parameter which takes into account mechanical mixing and diffusion:

$$\tilde{D} = D_m + \tilde{\alpha}_l v_p, \tag{36}$$

where D_m is molecular diffusion, $\tilde{\alpha}_l$ is the dynamic dispersivity, and v_p is the pore velocity. It is reasonable to suggest that TRINET is able to simulate transport in a porous medium aquifer with dispersivity $\tilde{\alpha}_l$ if the TRINET element dispersivity α_l is chosen to satisfy $\tilde{\alpha}_l = \alpha_l$. This equivalence between $\tilde{\alpha}_l$ and the TRINET element dispersivity α_l is verified for a 2D uniform quarter lattice described in Section 4.4.1 (Fig. 19). Here, an equivalent set of TRINET input parameters is developed for α_l. In the following example, the radial transport problem in section

4.4 is solved for in terms of aquifer dispersivity instead of the hydrodynamic dispersion. Note that molecular diffusion is assumed to be negligible. See *Javandel et al.* [1984] for details.

If molecular diffusion is negligible, equation (33) can be rewritten in terms of α_l, and v_p:

$$\frac{1}{r}\frac{\partial}{\partial r}\left(\alpha_l v_p r \frac{\partial C}{\partial r}\right) - v_p \frac{\partial C}{\partial r} = \frac{\partial C}{\partial t}. \tag{37}$$

As in equation (33), the aquifer is assumed to be a homogeneous, isotropic, confined aquifer of infinte horizontal extent with thickness $b = 1$ m. A solute with concentration C_0 is continuously injected into the aquifer through a fully penetrating well. If the injection rate is constant then for steady plane radial flow $v_p r$ is constant and simplifies Equation (37) to

$$\alpha_l v_p \frac{\partial^2 C}{\partial r^2} - v_p \frac{\partial C}{\partial r} = \frac{\partial C}{\partial t}. \tag{38}$$

Moench and Ogata [1981] give a Laplace transform solution for equation (38). Defining the dimensionless parameters $r_D = r / \alpha_l$, $t_D = Q\,t/2\pi b\phi\,\alpha_l^2$, and $C_D = C / C_0$ for radius, time and concentration, *Moench and Ogata* [1981] give the solution in the Laplace transform domain written in terms of Airy functions:

$$\mathscr{C}_D = \frac{1}{s}\exp\left[\frac{r_D - r_{Dw}}{2}\right]\frac{\mathrm{Ai(Y)}}{\mathrm{Ai(Y_0)}}, \tag{39}$$

where $\mathscr{C}_D$ is the Laplace transform of dimensionless (relative) concentration, s is the Laplace transform parameter, Ai(Y) is the Airy function, and

$$Y = s^{-2/3}\left(s\,r_D + \tfrac{1}{4}\right),$$
$$Y_0 = s^{-2/3}\left(s\,r_{Dw} + \tfrac{1}{4}\right),$$

where r_{Dw} is dimensionless well radius. A numerical inversion of the Laplace transform is required to obtain relative concentrations at specified times and radial distances. The FORTRAN program LTIRD provided by *Javandel et al.* [1984] is used to perform the inversion.

The TRINET solution is compared to LTIRD for the following problem. A solute with initial concentration $C_0 = 1$ is continuously recharged into an aquifer with thickness b = 1 m and porosity 0.2. The concentration of the recharge fluid is held constant at 1.0 and the rate of recharge Q is 0.1m^3/day.

TRINET is compared to the LTIRD solution at t = 10 years (Figs. 23—26). For convenience, the 40m quarter lattice in Section 4.4.1 (Fig. 19) is used, but apertures are altered slightly in order to match the aquifer porosity. Recall that in order for a 2D lattice with uniform grid spacing L to behave as a homogeneous aquifer with effective porosity ϕ in a radial flow field, the TRINET element apertures w must satisfy

$$\phi = 2w/L.$$

In this case the appropriate aperture choice is $w = \phi\,L/2 = (0.2)(1\mathrm{m})/2 = 0.1$ m. In addition, the contaminant source is assumed to be a point source so a single node can be used to

simulate the injection well. Since a quarter of the aquifer is modeled, the TRINET flow rate is set to $Q_{TRINET} = \frac{1}{4} Q$ or 0.025 m^3/day. TRINET solutions are compared to LTIRD for three dispersivities: $\tilde{\alpha}_l = 0.1$ m (minimal), $\tilde{\alpha}_l = 1.0$ m (mild), and $\tilde{\alpha}_l = 10$ m (moderate). The element dispersivities are set to $\alpha_l = \tilde{\alpha}_l$. Plots of relative concentrations for these dispersivities appear in Figs. 23-26. As expected, for nodes parallel to lattice elements, the concentration fronts arrive early, however for nodes along the diagonal, TRINET compares with the LTIRD solution quite well. When dispersivity is minimal, TRINET matches the LTIRD solution extremely well although the TRINET front along the diagonal appears to be slightly sharper between 25-30 m (Fig. 23). When the dispersivity is mild, TRINET also agrees with the analytical solution (see Fig. 24). When the dispersivity is moderate, however, the agreement is not as good (Fig. 25). This is most likely due to limitations of the mesh. At 10 years, the front has reached the outer boundary of the mesh and since the concentration is held constant at the boundary, differences between the solutions are to be expected (see Fig. 25).

In fact it looks as though the effects of the mesh boundaries are evident at around 20 m from the injection well and more obviously, at approximately 30 m away (Fig. 25). We can conclude that the 40 m radial mesh is adequate for modelling transport at early times, but not large enough to simulate an aquifer of infinite extent at later times when the front reaches distances beyond 10-15 m from the well. Ideally, a 60 m radius quarter mesh should be used to verify the case of moderate dispersivity. In order to investigate the possibility that TRINET dispersivity might require some adjustment, the LTIRD solution is also compared to the TRINET solution when $\alpha = 2\alpha_l = 20$ m. This is a plausible parameter choice given the correction factor of 2 for hydrodynamic dispersion in section 4.4. TRINET relative concentrations for the two dispersivities are plotted in Fig. 26. On observation, no correction is warranted.

These figures demonstrate that TRINET is quite accurate for grid nodes along the mesh diagonal. As in the longitudinal transport problem, solute appears to move faster for flowpaths parallel to the mesh. However, the plots suggest that no adjustment of element dispersivity is required (i.e., if all TRINET elements are given the same value for dispersivity, then element dispersivity and aquifer dispersivity are equivalent).

5. CONCLUSIONS

We have shown how TRINET can be used to model flow and transport in porous media. Only a slight modification of element properties is required in the case of a uniform lattice. For lattices with variable spacing, this adjustment is not as simple. However, a nested lattice is likely to be needed for modelling flow, not transport. TRINET is accurate for a range of inputs for flow in a confined aquifer and for flow in a leaky aquifer. In addition, we have demonstrated that TRINET can be used to closely simulate longitudinal transport and radial transport (under steady flow) for porous media. The simulation is accurate even when a fairly coarse, simple mesh such as the uniform lattice is used. Some care must be taken in handling the effects of grid orientation for 1D transport by either using a diagonal mesh or correcting the porosity appropriately for a linear mesh. TRINET can be computationally less expensive than evaluating the analytical solution directly. For example, in the radial transport problem, it was faster to simulate transport with TRINET than to evaluate the analytical solution directly. Equivalence expressions for permeability, storativity, dispersion and porosity have been developed and verified with TRINET.

For flow in a confined aquifer with unit thickness b, permeability $\tilde{K}$ or transmissivity $\tilde{T}$, and storativity $\tilde{S}_s$, a two-dimensional uniform lattice with grid spacing L can be used to model flow if element transmissivity is chosen to satisfy $\tilde{T} = Tb/L$ and element storativity and aperture are chosen to satisfy $\tilde{S}_s = 2S_s\ w/L$. For flow in a leaky aquifer with permeability $\tilde{K}$ (transmissivity $\tilde{T}$) and storativity $\tilde{S}_s$, a three-dimensional uniform lattice with grid spacing L can be used to model flow if element transmissivity, aperture and storativity are chosen to satisfy $\tilde{T} = Twb/L^2$ and $\tilde{S}_s = 3S_s(w/L)^2$. By observation, these expressions suggest a generalization for an n-dimensional uniform rectangular lattice:

$$\tilde{T} = T/L^{n-1} \text{ if } w = b = 1,$$

$$\tilde{S}_s = nS_s(w/L)^{n-1}.$$

For flow and transport, if the flow is parallel to one of the element orientations (i.e., there is flow along elements in one particular direction and no flow in the other elements), the effective porosity is given by $\phi = (w/L)^{n-1}$ assuming $w = b$. If the flow direction is such that most of the elements participate in flow and transport, the effective porosity is given by $\phi = n(w/L)^{n-1}$. For dispersion, the effective hydrodynamic dispersion, is given by $\tilde{D} = D/n$ regardless of the direction of flow. This suggests that for modelling transport in a heterogeneous flow field, the effect of lattice orientation on the effective porosity (and hence pore velocity) is expected to be small since most of the element participate in flow and transport. The linear lattice is recommended in this case due to its ease of construction and in the specification of TRINET flow and transport boundary conditions.

APPENDIX 1.
INJECTION RATE FOR THE RADIAL TRANSPORT PROBLEM

In order to correctly assign flow rates and verify that the four nodes collectively behave as a 1 m radius well for steady state flow, Thiem's equation is applied twice in the following manner. Using Thiem's equation,

$$Q = -2\pi \tilde{T} \frac{(h_2 - h_1)}{\ln(r_2/r_w)}, \tag{A1}$$

the flow rate in TRINET (Q_{TRINET}) required to achieve a specified head boundary condition can be determined if the effective well radius is known. Conversely, the effective well radius for a TRINET lattice can be inferred by applying the same prescribed head boundary conditions and setting $Q = Q_{TRINET}$ in Thiem's equation and solving for the effective well radius. First the head boundary conditions are imposed with $h_1 = 20$ m at $r_w = 1$ m and h_2 0 m at $r_2 = 20$ m. The combined flow rate at the four well nodes calculated by TRINET is $Q_{TRINET} = 2.1\text{e-}06$ m^3/s. Next, imposing a flow boundary condition at each of the injection wells with each well node assigned a flow rate of $q_{node} = \frac{1}{4} Q_{TRINET} \cong 5.25\text{e-}07$ m^3/s, the following pressures were observed: $h_1 =$ 20.07 m at $r_w = 1$ m and $h_2 = 0$ m at $r_2 = 20$ m. Using Theim's equation gives an effective well radius of

$$r_w = \frac{r_2}{\exp\left(-2\pi\tilde{T}(h_2 - h_1)/Q_{TRINET}\right)} = 0.99 \text{ m.}$$

which is quite close to 1 m. Hence, this well configuration is sufficient for simulating flow with a 1 m radius well. The TRINET steady state pressure at each well node is 21.588 m so equivalently, the head at the well nodes can be fixed at 21.588 m such that the flow rate from each node is exactly 1/8 of the original flow rate.

APPENDIX 2.
NUMERICS SENSITIVITY STUDY (Pulse Injection Test)

This appendix summarizes results from a sensitivity study that was conducted in order to model a simple transport problem. Due to computational constraints, we use a new version of TRINET, the finite element code TRIPOLY [*Birkholzer and Karasaki*, 1996]. TRIPOLY has several advantages over TRINET, including the following.

- An option to specify an element dispersivity instead of a lumped dispersion coefficient in the element file.

- An improved adaptive gridding procedure that reduces numerical dispersion by introducing new dispersive nodes either when elements with low velocities are detected or in the vicinity of steep concentration gradients.

- An automatic time step control that reduces computational inefficiency by reducing the time step size so that fewer advective nodes are added. Note that if the time step is too large, too many new nodes are added and solving the transport equation becomes inefficient.

The numerics control variables examined in this appendix, DEPS, DCDIF, DCON, and DCOFF, determine how many new nodes are added during adaptive gridding. These variables are described in *Birkholzer and Karasaki* [1996]. The focus in this section is to determine optimal values for these variables in order to accurately and efficiently model a natural gradient tracer experiment in the saturated zone of a heterogeneous aquifer [*Beach et al.*, 1996]. Previous studies of the site suggest a porosity of 0.35 and the dispersivity is estimated to be approximately 5m [*Adams and Gelhar*, 1992]. Hydraulic conductivity ranges over several orders of magnitude (1e-06 cm/s to 1.0 cm/s). Piezometric head data suggests that the natural gradient (5e-03) is generally northward, but varies in magnitude and direction in time [*Beach et al.*, 1996]. Tracer is injected at a well approximately 350m upstream from the furthest downstream monitoring well. Tracer is injected for 48 hours and the data consist of concentrations (five snapshots showing the spatial distribution of tracer) taken over the course of the experiment (approximately 440 days).

The task of modelling this experiment is simplified by simulating transport in a 2D vertical section along the middle of the monitoring array. This also corresponds to the center of the tracer plume. Boundary conditions are specified in order to match the observed hydraulic gradient and to achieve a one dimensional flow field. To model the pulse injection, a solute of fixed concentration (unit concentration) is injected at a constant rate for approximately 48 hours after which the well is turned off for the remainder of the experiment. The injection rate is specified to be small enough and the hydraulic conductivity large enough so that the injection well does not significantly affect the one-dimensional flow field. Since the pulse injection introduces a steep concentration gradient, we are interested in determining appropriate values for DCON and DCOFF, the threshold concentration gradients at which nodes are added and removed, respectively, to accurately model advection. In addition, the pressure gradient is not very large, therefore some mesh elements may have low velocities and selecting an appropriate value for DCDIF, the threshold concentration gradient at which nodes are added to accurately model diffusion, is also of interest. Table 3 summarizes the values for each variable that are examined in this sensitivity study.

Table 3. Values of TRIPOLY control parameters for each factor level.

FACTOR	VARIABLE NAME	LEVEL			
		0	1	2	3
A	DEPS	0.001	0.1	1.0	--
B	DCDIF	0.1	0.01	0.001	1.E-04
C	DCON	0.01	0.001	1.E-04	--
	DCOFF	5.E-03	5.E-04	5.E-05	--

Two sets of runs are performed. In the first set, the value is changed for a single factor with other factor levels held at base values (level 0). In general, higher levels of A (DEPS) have no effect when B (DCDIF) and C (DCON, DCOFF) are held at base levels, so TRIPOLY seems to be relatively insensitive to changes in DEPS. In the second set, levels of factors B and C are changed simultaneously with A held at base level. Some of these runs are ranked by numerical accuracy relative to the base case A0B0C0.

1. **A0B2C0 A0B2C1 A0B2C2 A0B3C0 A0B3C1 A0B3C2**
2. **A0B1C1 A0B1C2**
3. **A0B1C0**
4. **A0B0C2 A0B0C1**
5. **A0B0C0 A1B0C0**

Runs listed in the same line are more or less equivalent (less than 2% difference in peak concentration). Runs in line 1 versus line 3 differ by about 10%, runs in lines 3 and 5 differ by about 20-25% and runs in lines 4 and 5 differ by about 15%. Differences between runs in lines 2 and 3 are difficult to estimate because these runs produce similar breakthrough curves. Note that these statistics are intended for use primarily to rank the more accurate runs. Roughly, the runs in line 1 are preferable compared to the runs in lines 2 and 3. The runs in lines 4 and 5 are not recommended since the relative error (relative to the base case) is more than 10%.

Tables 4 and 5 below give run time required (in seconds) for the runs listed above and run times as a percentage increase over the base case. Note that factor A (DEPS) is omitted.

Table 4. Run time in seconds for A=0 cases.

FACTOR	DURING INJECTION			AFTER INJECTION		
C	0	1	2	0	1	2
B=0	30	29	33	29	33	45
B=1	31	34	38	33	38	52
B=2	33	38	45	38	50	72
B=3	33	35	45	53	60	88

Table 5. Percent increase in run time compared to case A0B0C0, for other A=0 cases.

FACTOR	DURING INJECTION			AFTER INJECTION		
C	0	1	2	0	1	2
B=0	--	-3	10	--	14	55
B=1	3	13	27	14	31	79
B=2	10	27	50	31	72	148
B=3	10	17	50	83	107	203

These results indicate that the most economical of the sufficiently accurate runs performed so far is A0B2C0 so we recommend setting DEPS=1E-03, DCDIF=1E-03, DCON=1E-02 and DCOFF=5E-03.

ACKNOWLEDGMENT

This work was supported in part by the Director, Office of Energy Research, Office of Basic Energy Sciences, of the U.S. Department of Energy under Contract No. DE-AC03-76SF00098 and in part by the Air Force Office of Scientific Research, USAF, under grant/contract number FQ8671-96-0-1169. We are grateful to Andrew Cohen and Janet Jacobsen for their reviews of this work. We thank Thomas B. Stauffer for providing the Columbus Air Force Base tracer data set described in the appendix. The views and conclusions contained herein are those of the authors and should not be interpreted as necessarily representing the official policies or endorsements, either expressed or implied, of the Air Force Office of Scientific Research or the U.S. Government.

REFERENCES

Adams, E. E. and L. W. Gelhar. Field study of dispersion in a heterogeneous aquifer. 2. Spatial moments analysis. *Water Resources Research*, 28(12), 3293-3307. 1992.

Beach, J., D. Fryar, H. Rifai, K. Appling, and T. B. Stauffer. Evaluation of natural attenuation of organic tracers at the MADE site using the Bioplume II transport model. Armstrong Laboratory, AL/EQ-TR-1996-0027. 1996.

Birkholzer, J. and K. Karasaki. FMG, RENUM, POLY, TRIPOLY: Suite of programs for calculating and analyzing flow and transport in fracture networks embedded in porous matrix blocks. Lawrence Berkeley National Laboratory. Berkeley, California. Technical Report #39387-000. 1996.

Boggs, J.M., S.C. Young and L.M. Beard. Field study of dispersion in a heterogeneous aquifer. 1. Overview and site description. *Water Resources Research*, 28(12), 3281-3291. 1992.

Carslaw, H. S. and J. C. Jaeger. *Conduction of Heat in Solids*. Clarendon Press, Oxford, 1946.

Doughty, C. Estimation of hydrologic properties of heterogeneous geologic media with an inverse method based on iterated function systems. PhD thesis, University of California. 1995.

Fetter, C.W. *Applied Hydrogeology, 3rd ed.* Macmillan College Publ. Co., New York, 1994.

Hantush, M.S. and C.E. Jacob. Non-steady radial flow in an infinte leaky aquifer, Trans., Amer. Geophys. Union, 36(1), 95-100, 1955.

Jaeger, J.C. Numerical values for the temperature in radial heat flow. *J. Math. Physics*. (34), 316-321. 1956.

Javandel, I., C. Doughty, and C. Tsang. *Groundwater Transport: Handbook of Mathematical Models*. AGU, 1984.

Karasaki, K. Well test analysis in fractured media. PhD thesis, University of California, 1987.

Karasaki, K. A new advection dispersion code for calculating transport in fracture networks. Technical report, Lawrence Berkeley National Laboratory, 1986-1987 Annual Report LBL-22090, 1987.

Moench, A.F. and A. Ogata. A numerical invesion of the Laplace transform solution to radial dispersion in a porous medium. *Water Resources Research*, 17(1), 250-252, 1981.

Ogata, A. and R. B. Banks. A solution of the differential equation of longitudinal dispersion in porous media. U. S. Geological Survey Professional Paper 4111-A, 1961.

Ozisik, M.N. *Heat Conduction, 2nd ed.* Wiley, New York, 1993.

Segan, S. and K. Karasaki. TRINET: A flow and transport code for fracture networks. User's manual and tutorial. Lawrence Berkeley National Laboratory, Berkeley, California, Technical report #LBL-34839, 1993.

Theis, C.V. The relation between the lowering of the piezometric surface and the rate and duration of discharge of a well using ground-water storage. Trans., Amer. Geophys. Union, 16, 519-524, 1935.

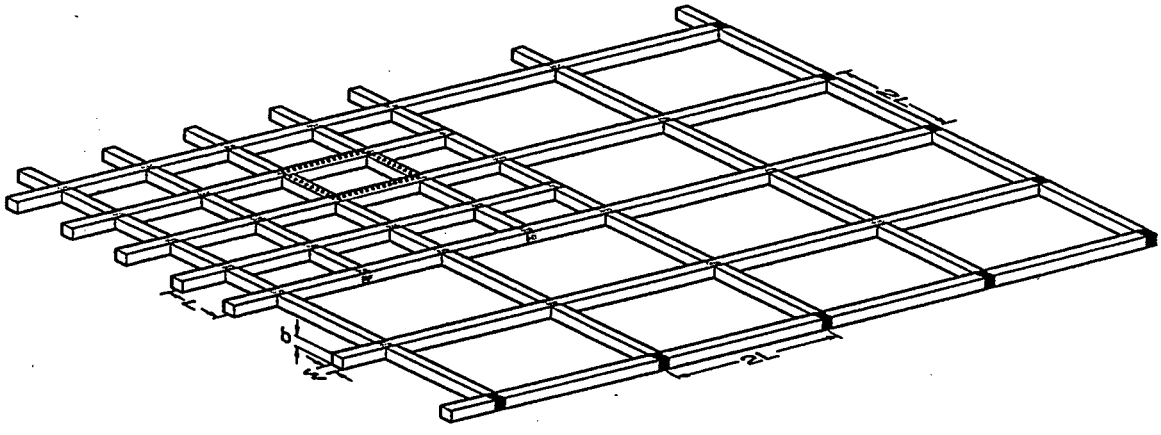

Fig. 1. Schematic diagram of a two-dimensional TRINET lattice.

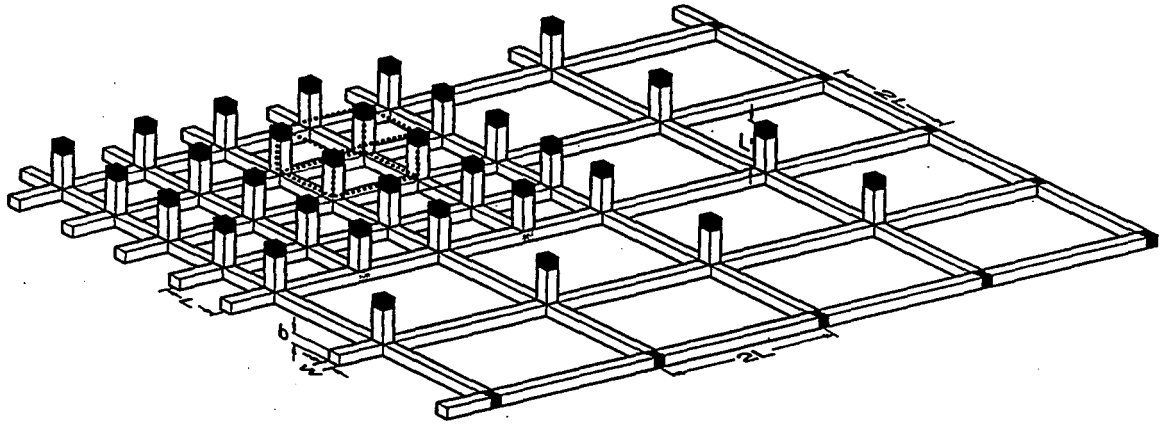

Fig. 2. Schematic diagram of a quasi three-dimensional TRINET lattice.

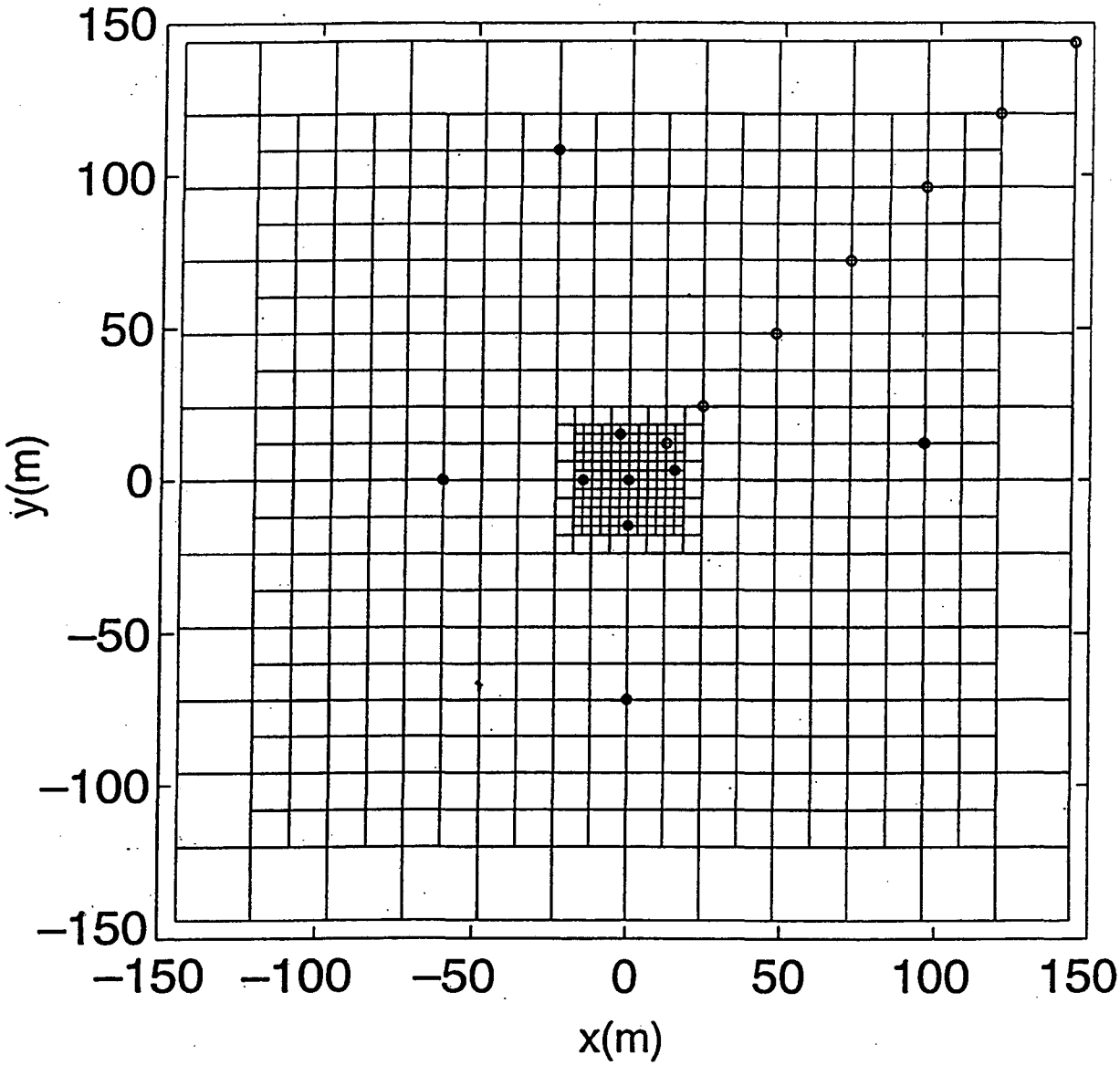

Fig. 3. TRINET lattice used for verification calculations.

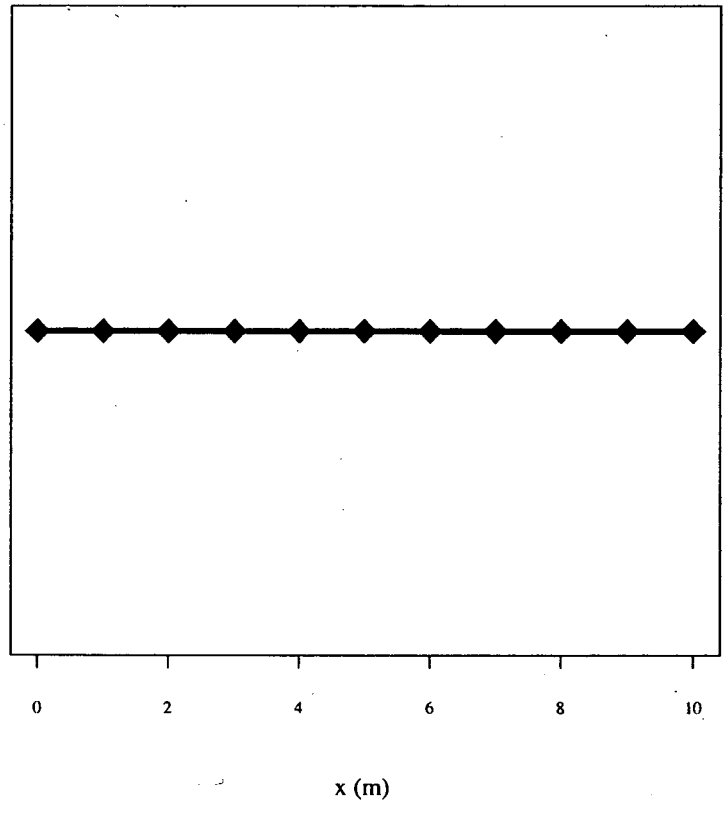

Fig. 4. TRINET 1D lattice for 1D transport through a pipe.

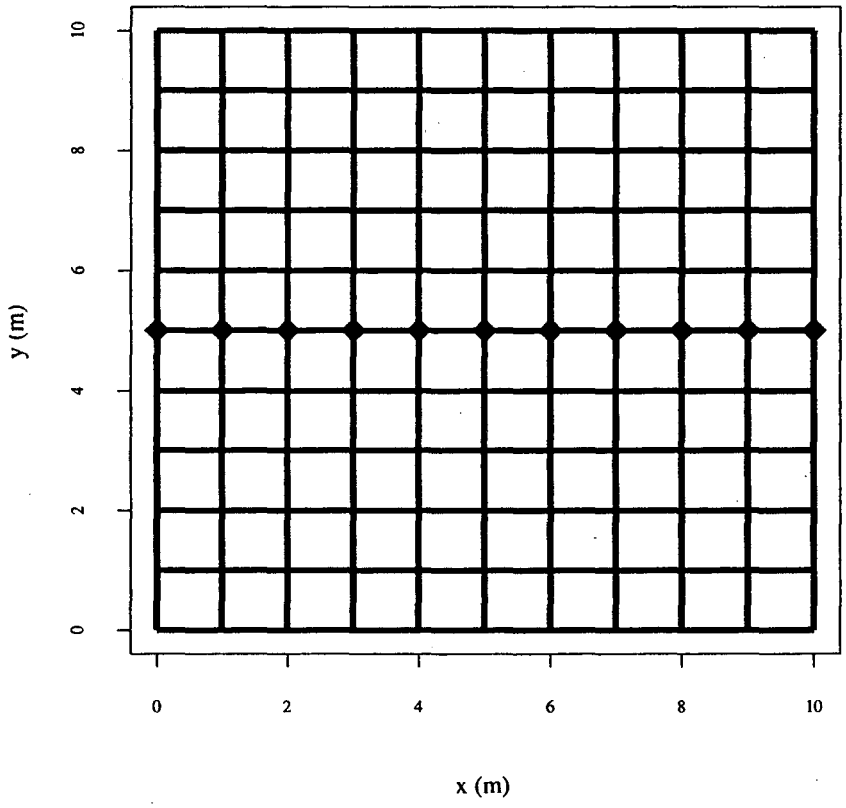

Fig. 5. TRINET 2D uniform linear lattice for 1D transport problem.

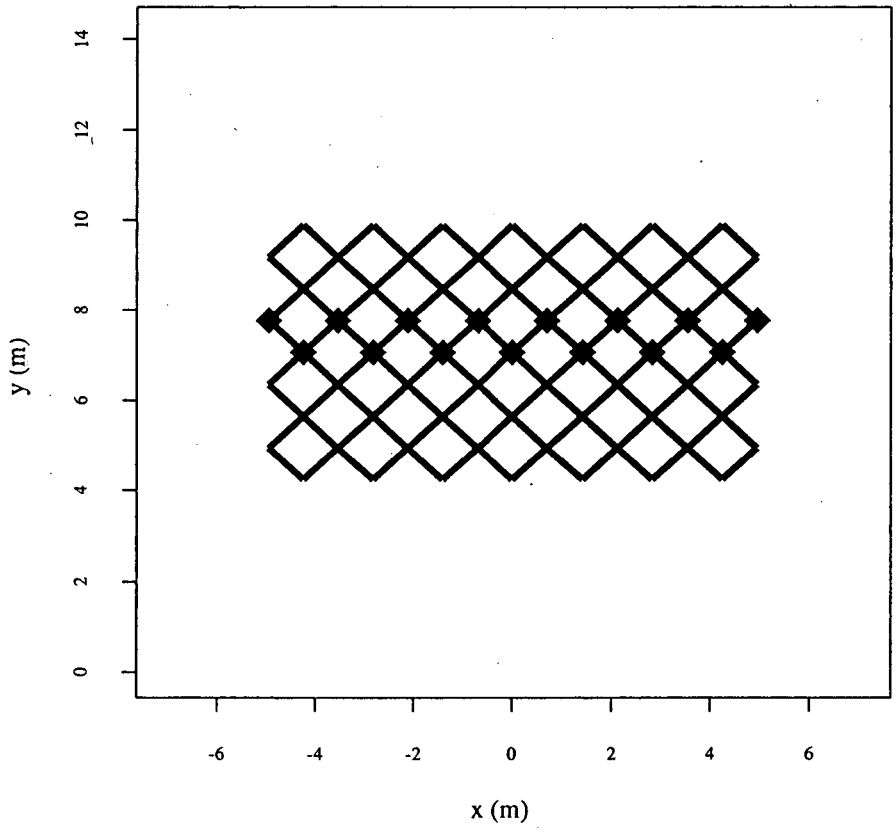

Fig. 6. TRINET 2D diagonal lattice for the 1D transport problem.

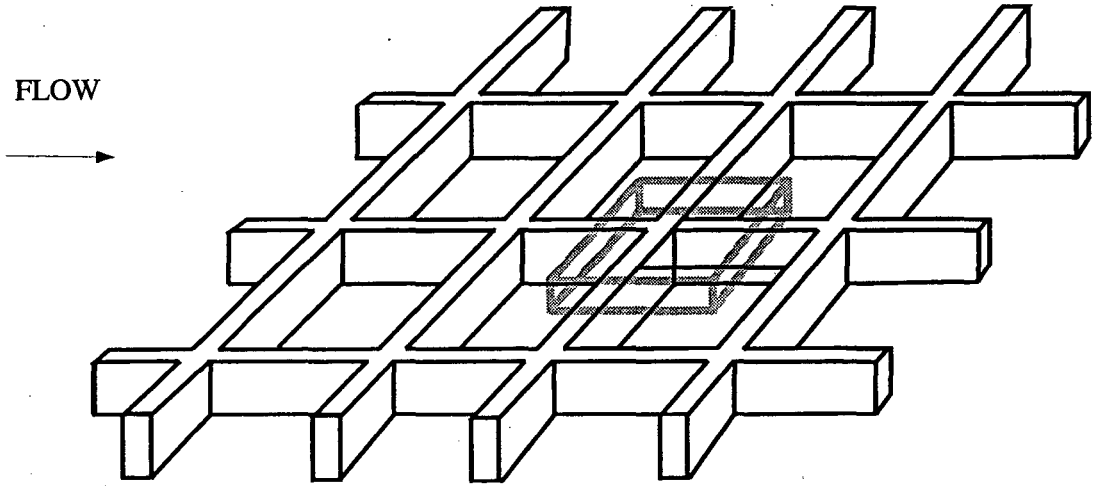

Fig. 7. Schematic diagram of a unit cell in the two-dimensional "linear" TRINET lattice shown in Fig. 5.

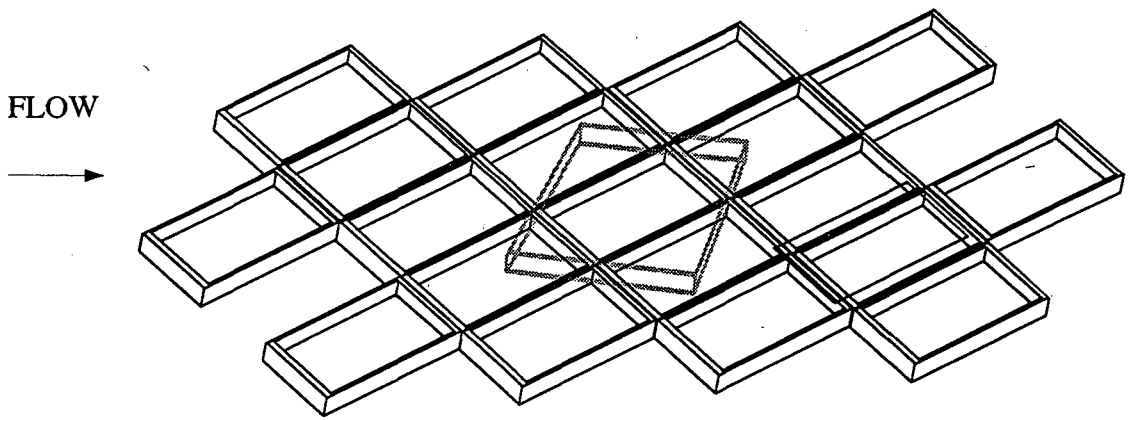

Fig. 8. Schematic diagram of a unit cell in the two-dimensional "diagonal" TRINET lattice shown in Fig. 6.

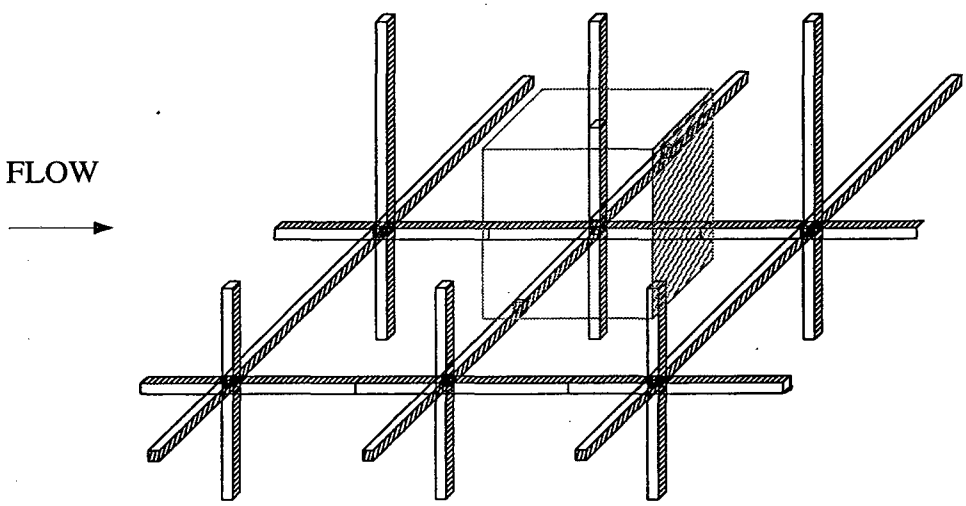

Fig. 9. Schematic diagram of a unit cell in the three-dimensional TRINET lattice.

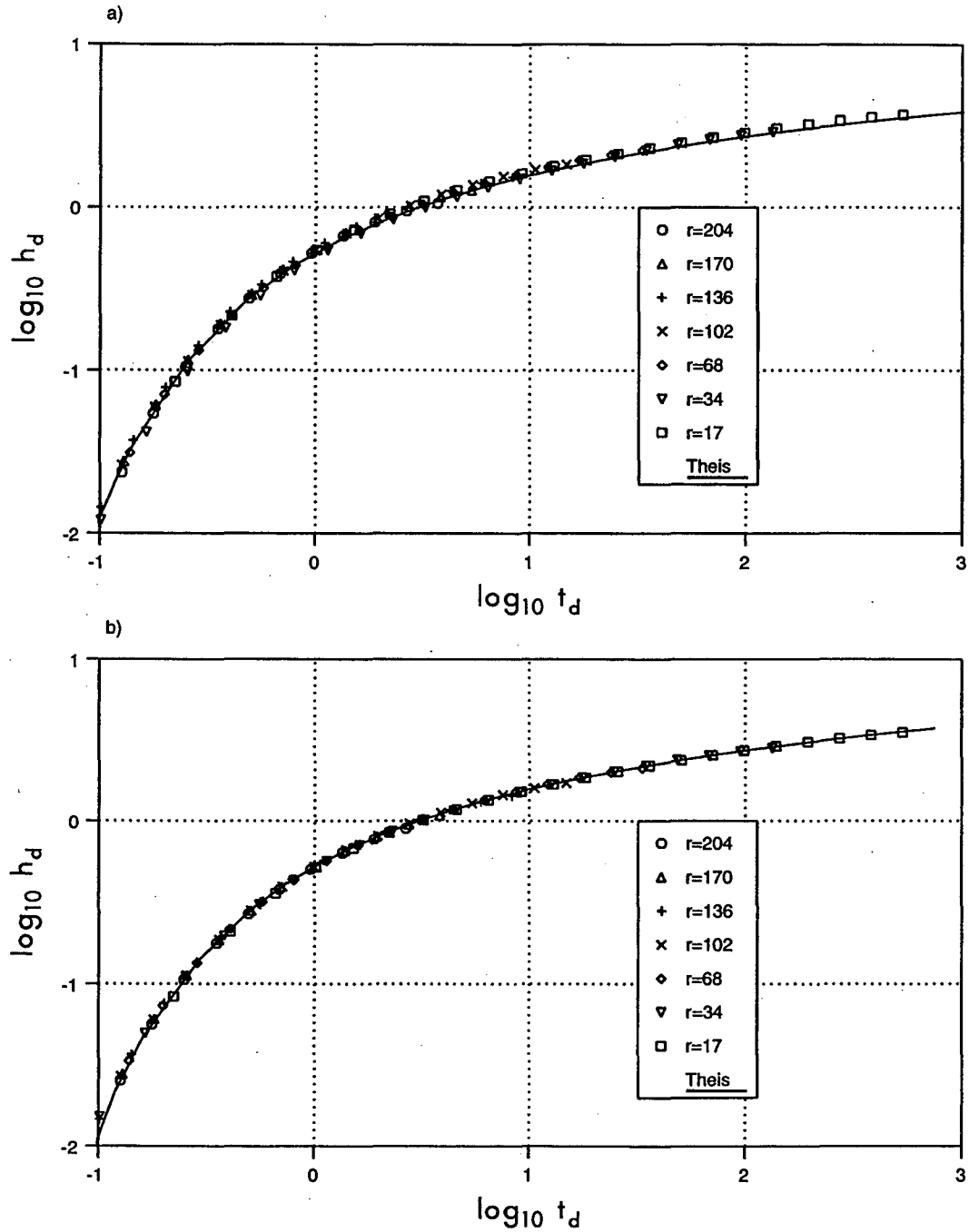

Fig. 10. TRINET comparison with *Theis*[1935] solution: a) using the lattice shown in Fig. 2; b) using a finer lattice.

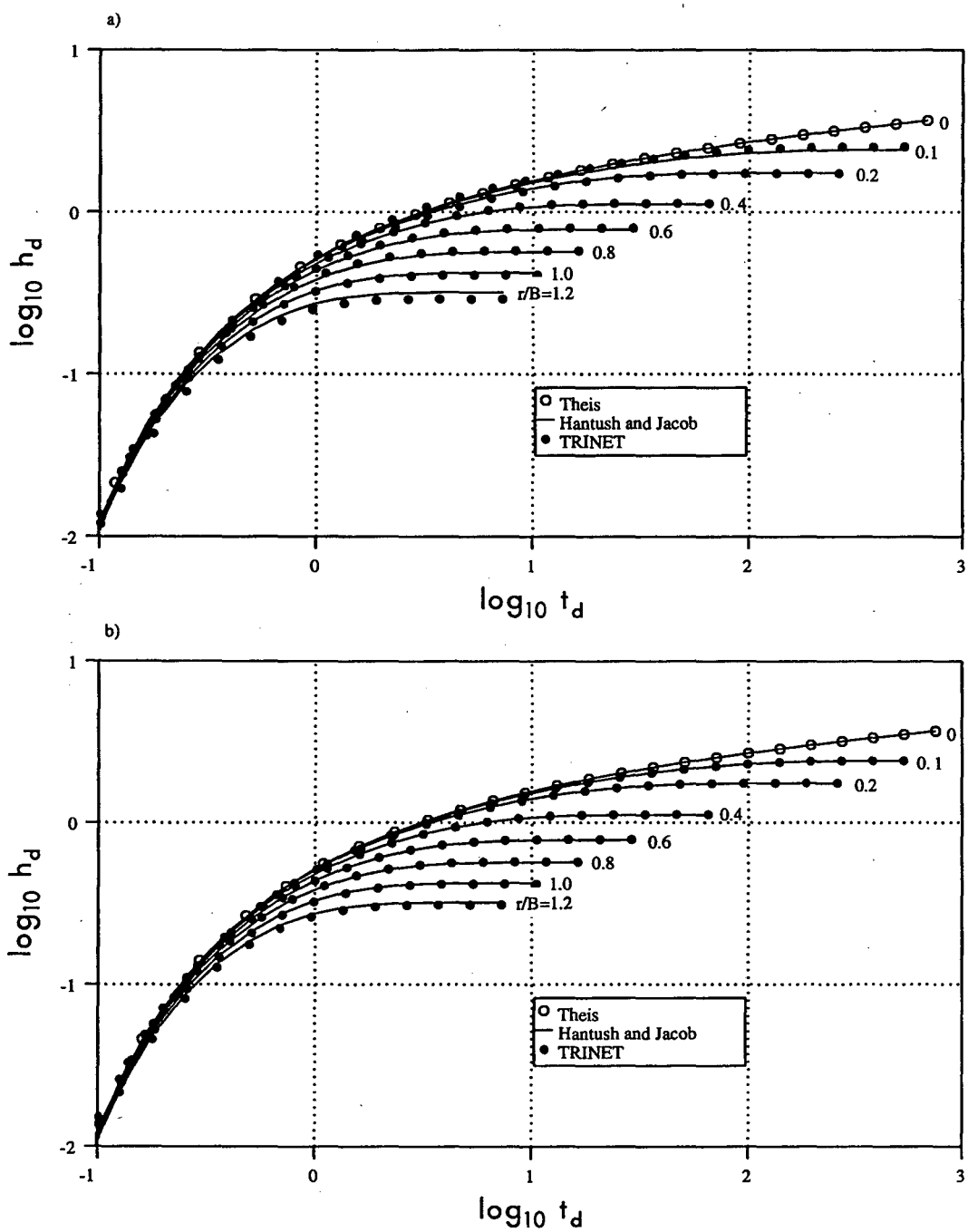

Fig. 11. TRINET comparison with *Hantush and Jacob*[1955] solution: a) using the lattice spacing shown in Fig. 2; b) using a finer lattice.

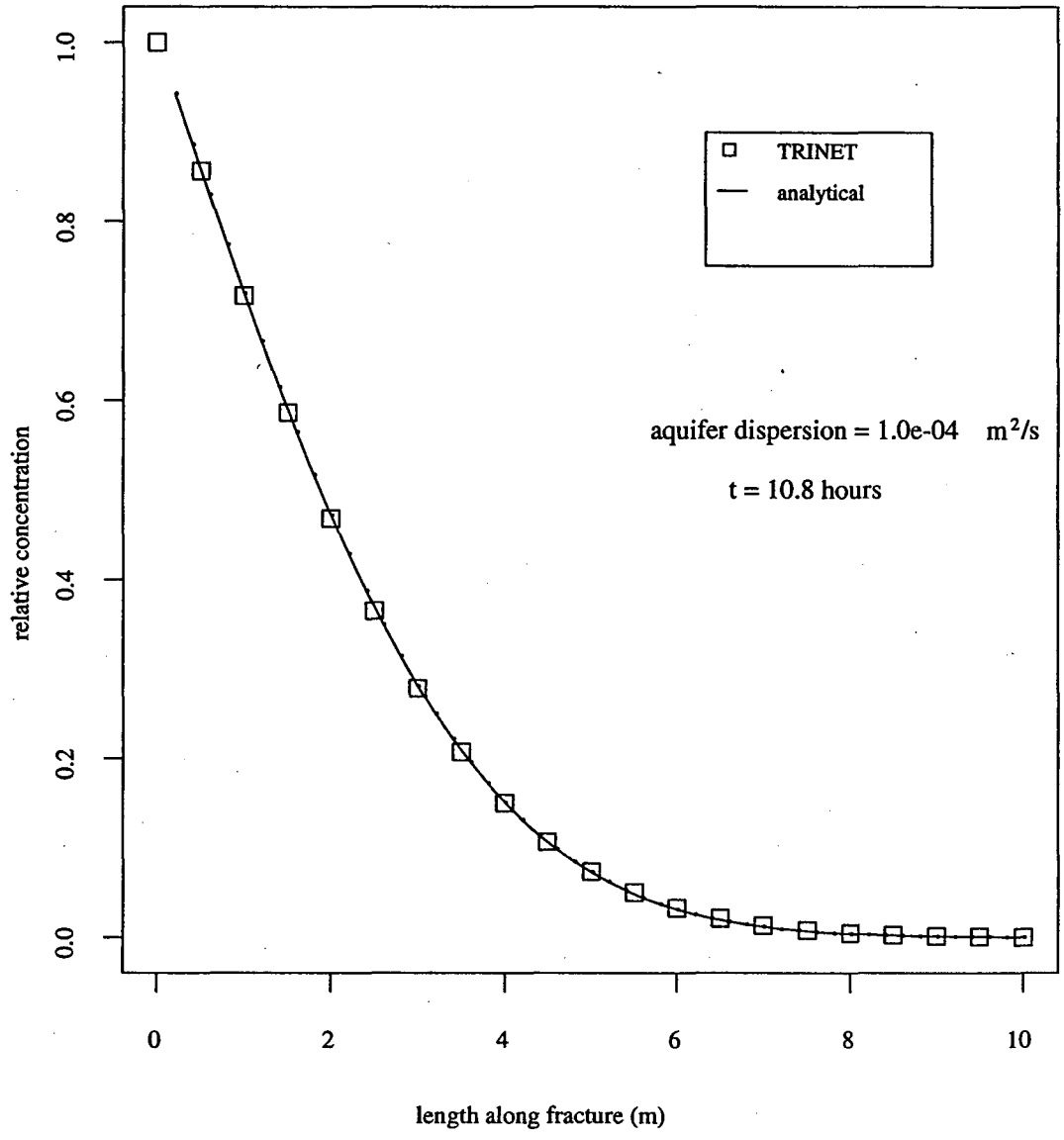

Fig. 12. TRINET comparison with solution to advection-dispersion equation for the diffusion only case using a 1D lattice.

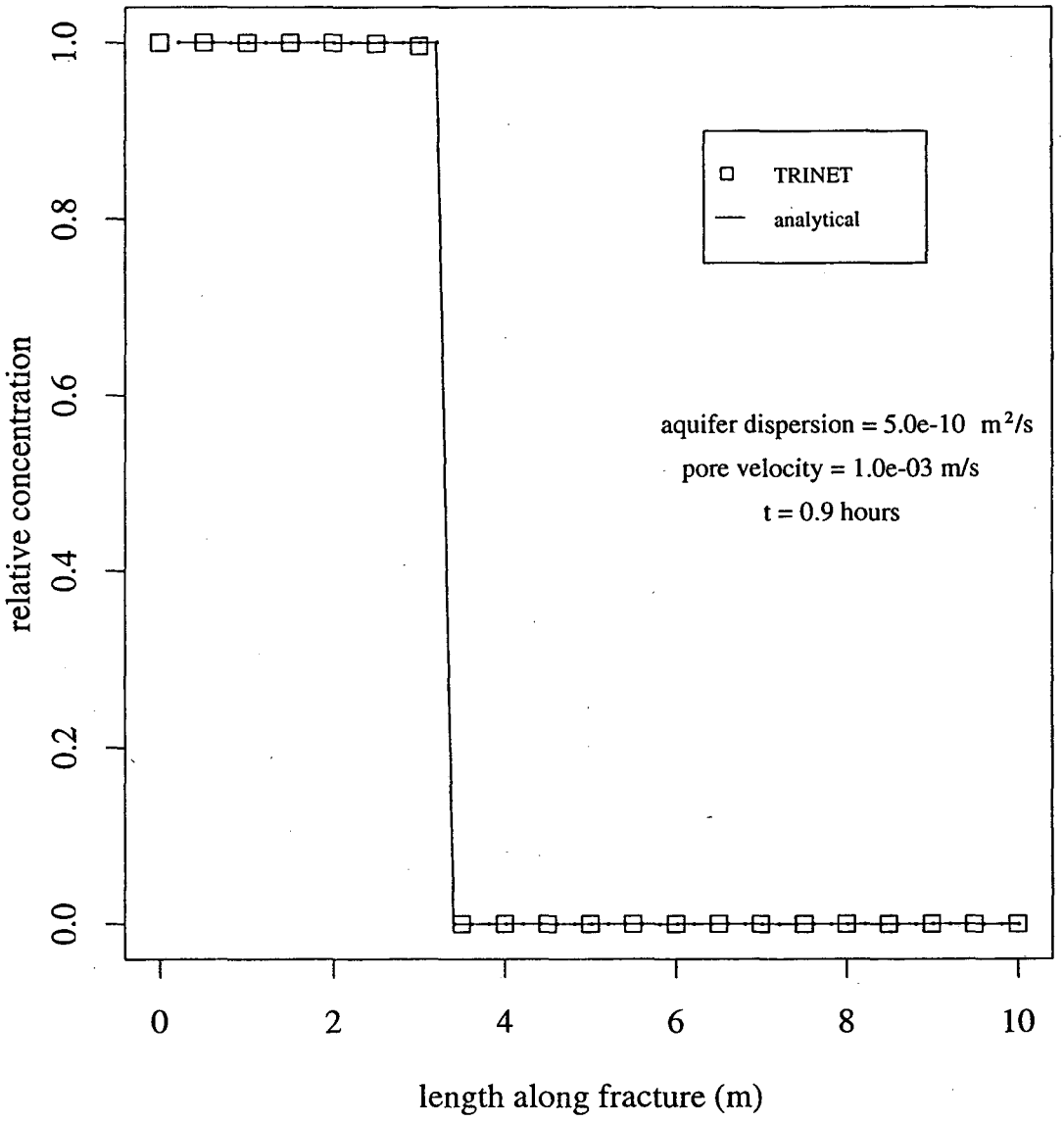

Fig. 13. TRINET comparison with solution to advection-dispersion equation for the advection only case using a 1D lattice.

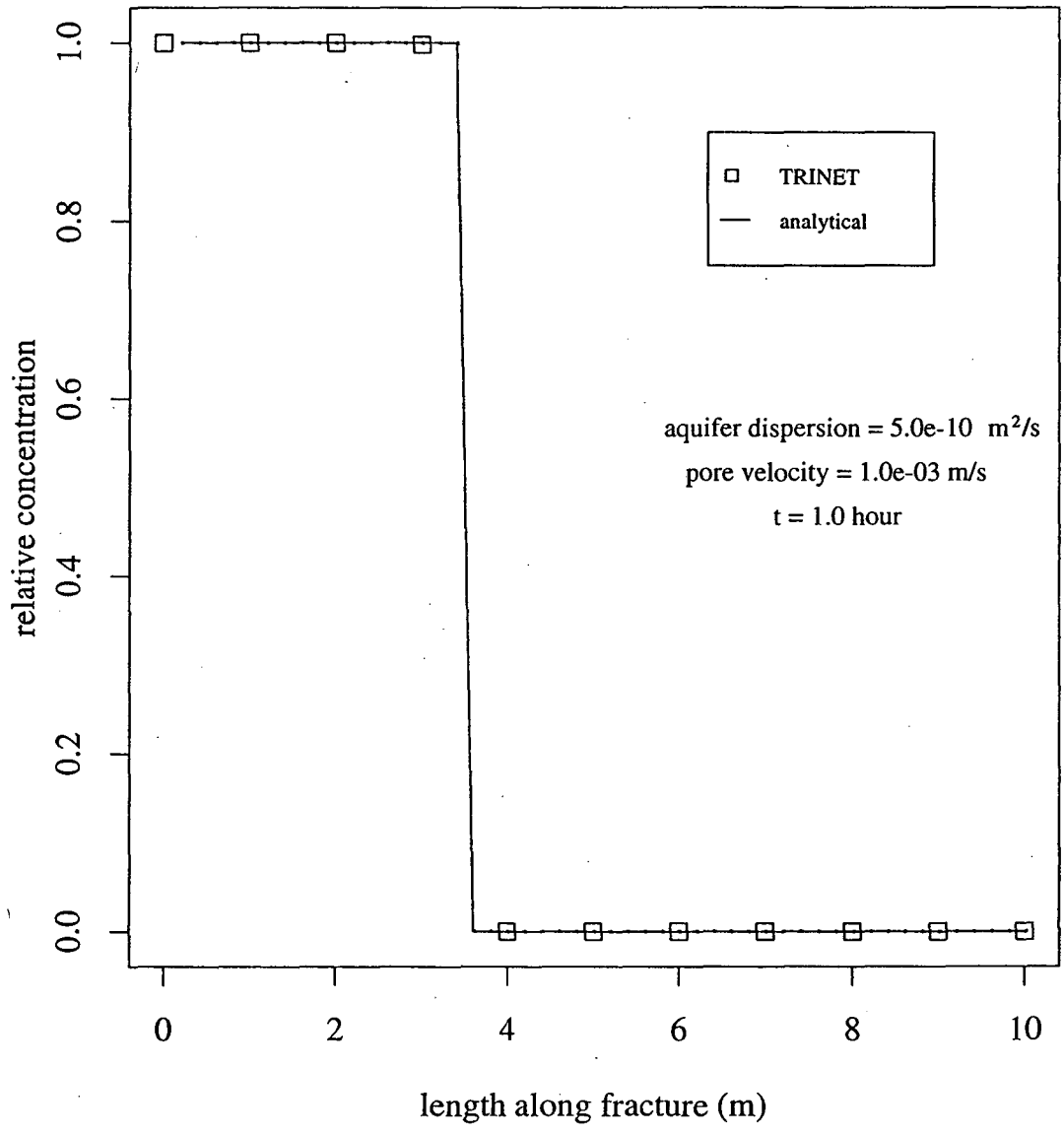

Fig. 14. TRINET comparison to analytical solution of the advection-dispersion equation for the advection-only case using the linear lattice.

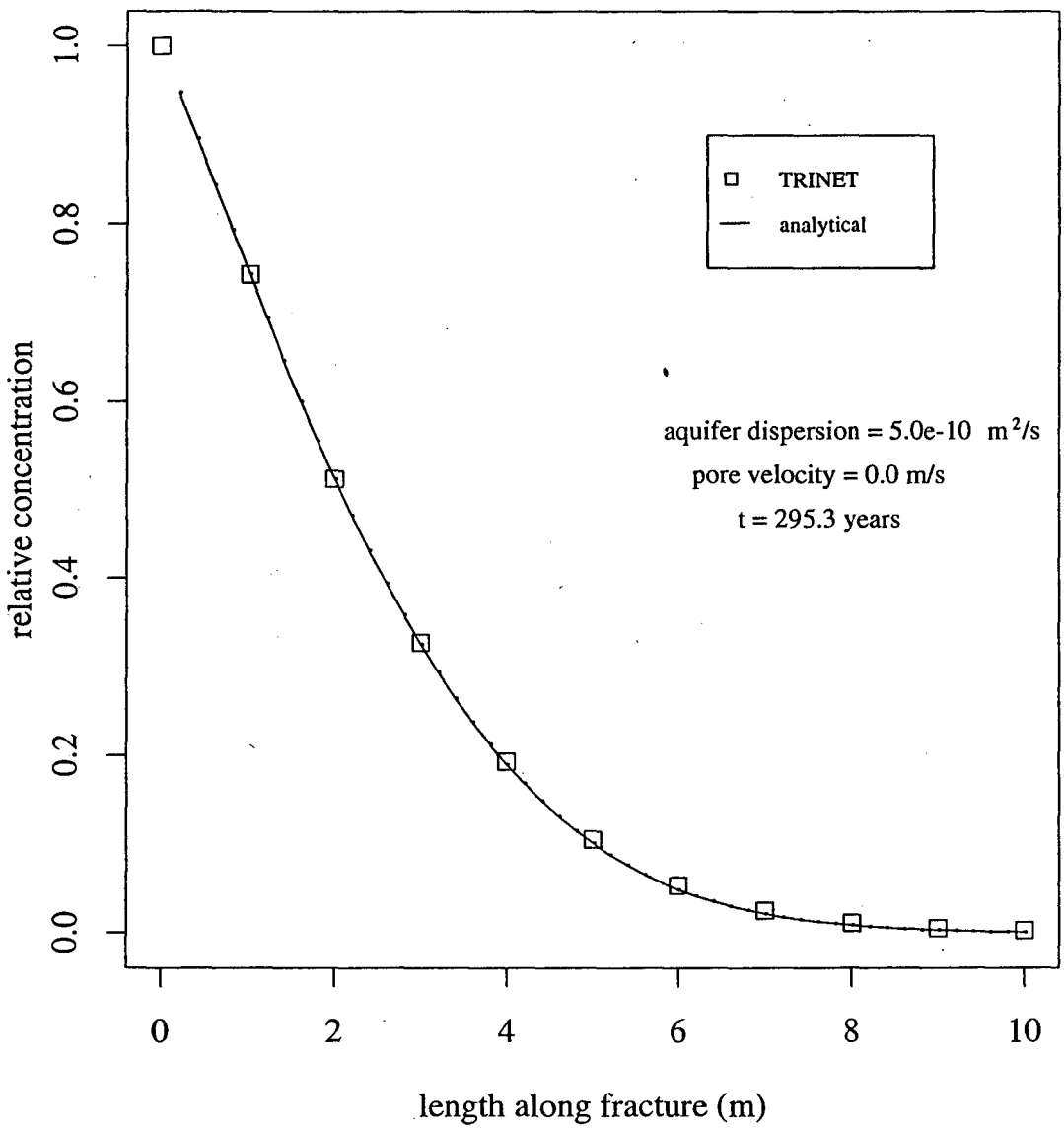

Fig. 15. TRINET comparison to analytical solution of the advection-dispersion equation for the diffusion-only case with the linear lattice.

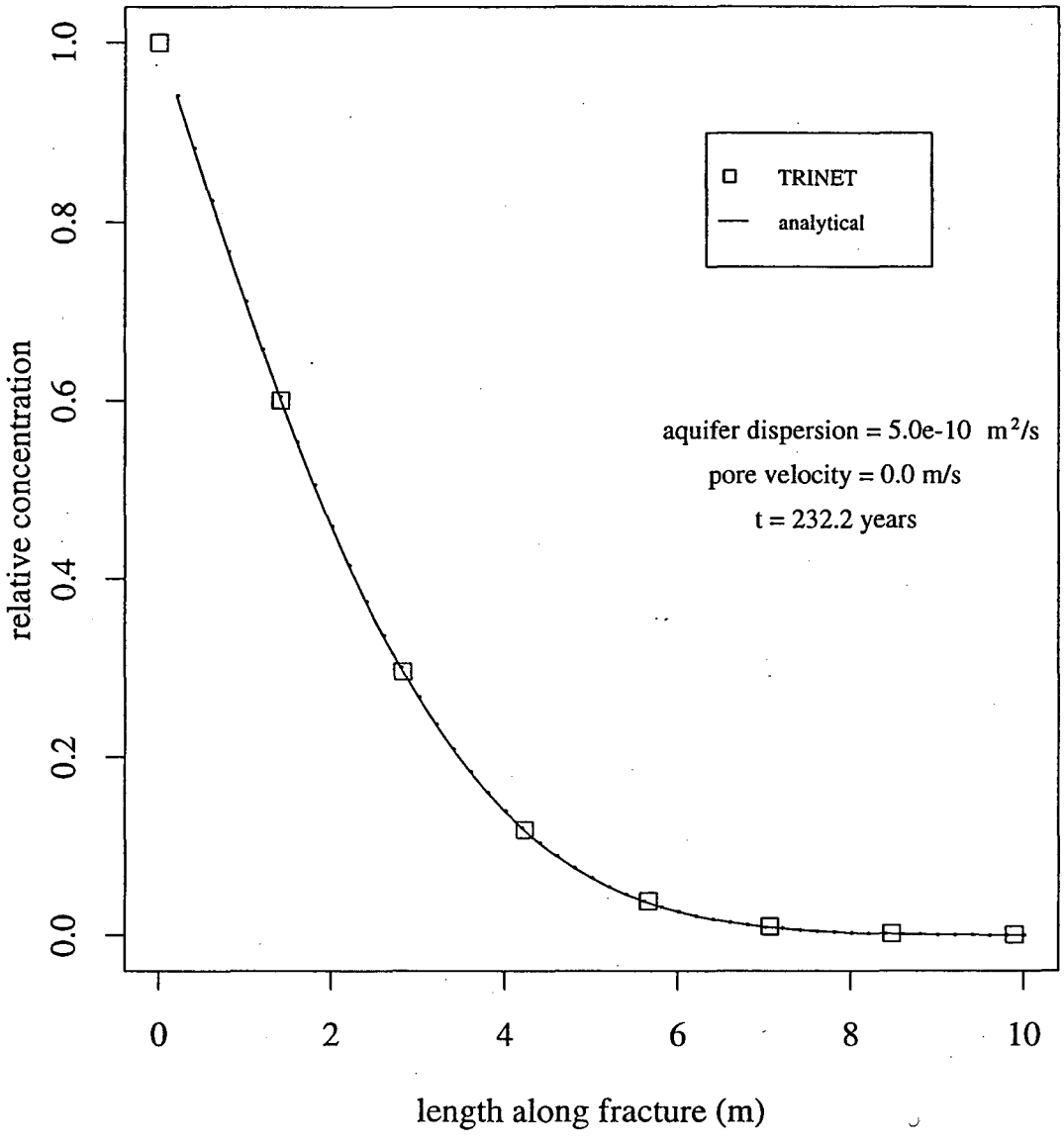

Fig. 16. TRINET comparison to analytical solution of the advection-dispersion equation for the diffusion-only case with the diagonal lattice.

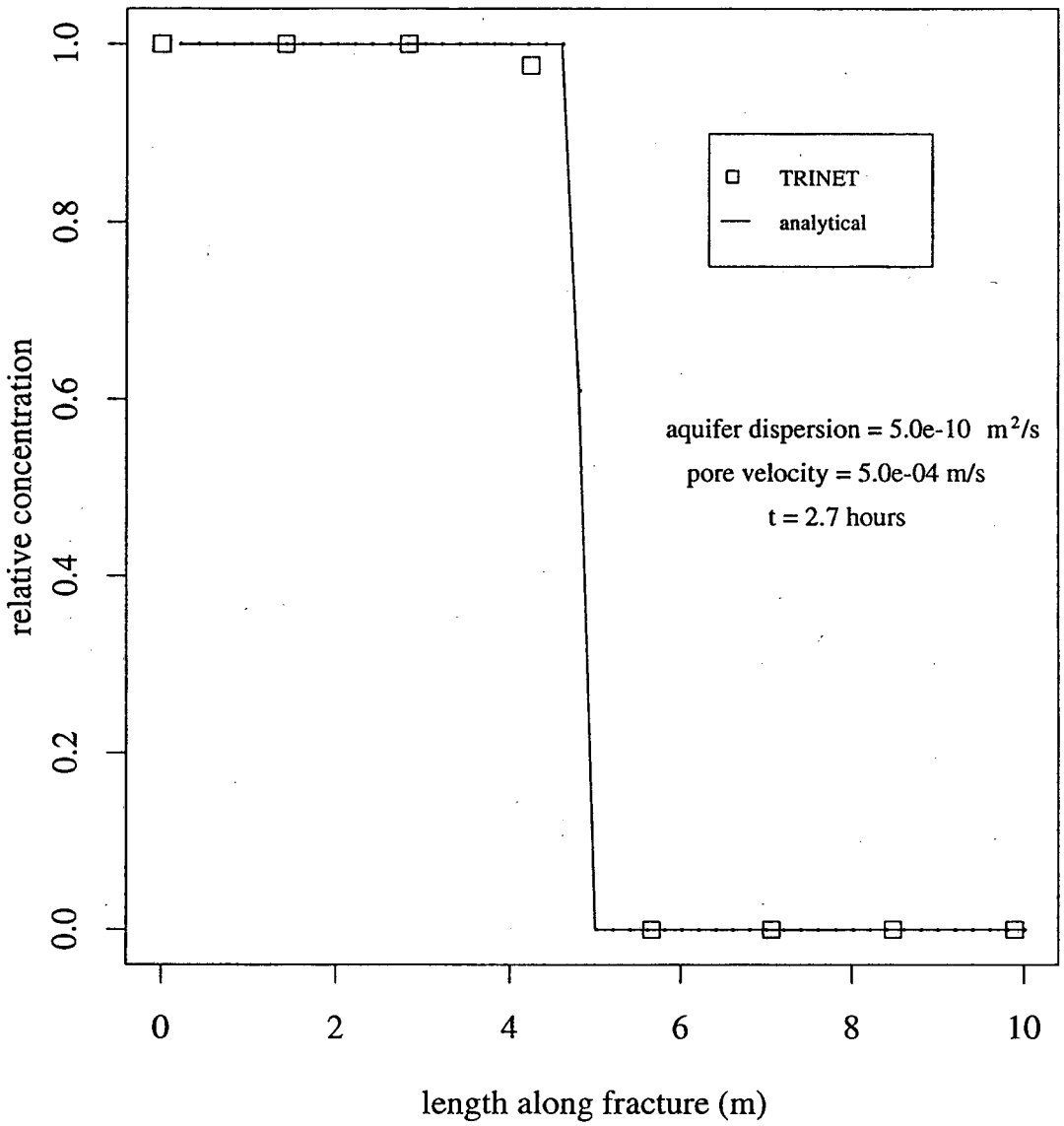

Fig. 17. TRINET comparison to analytical solution of the advection-dispersion equation for the advection only case using the diagonal lattice.

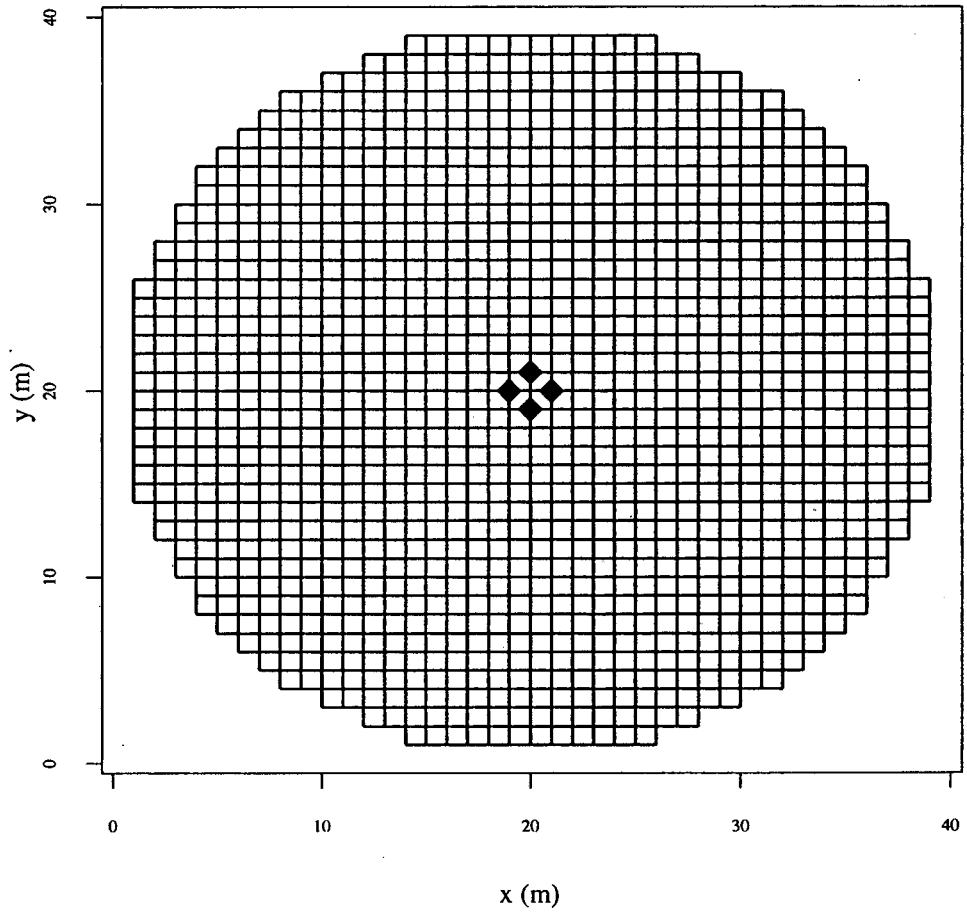

Fig. 18. TRINET lattice used for the radial transport problem.

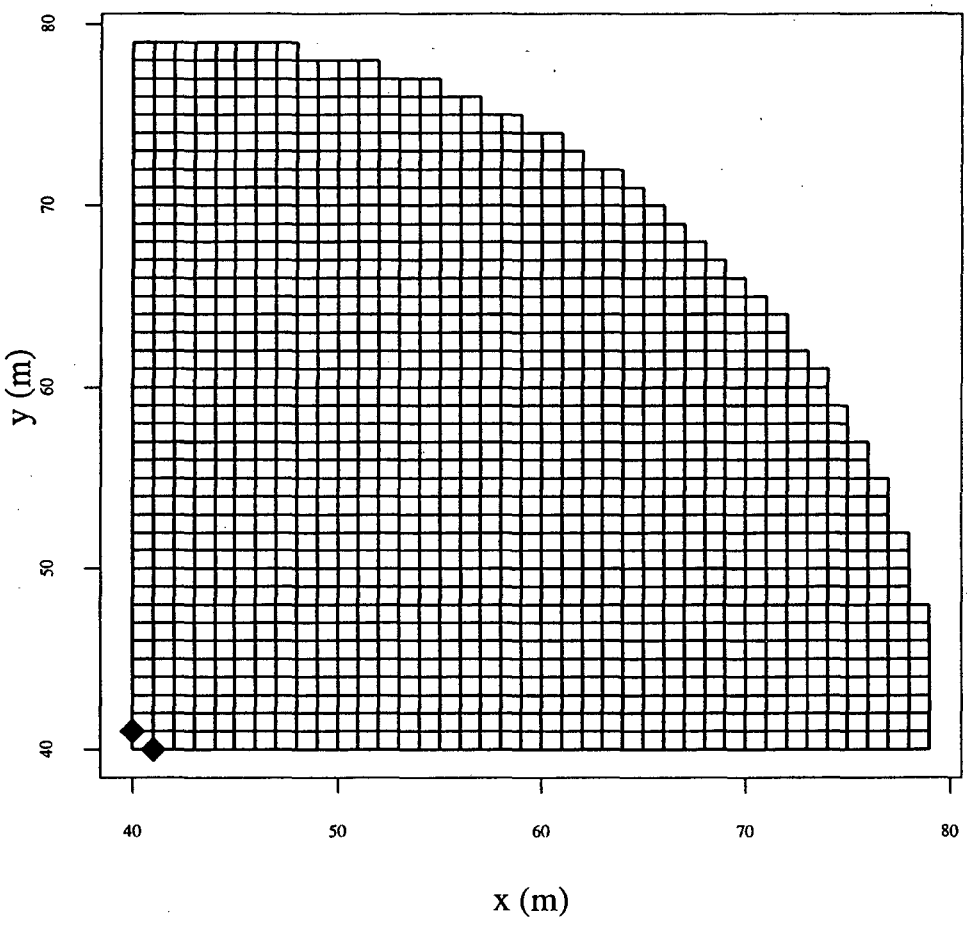

Fig. 19. TRINET quarter lattice used for the radial transport problem TRINET well nodes marked by filled diamonds.

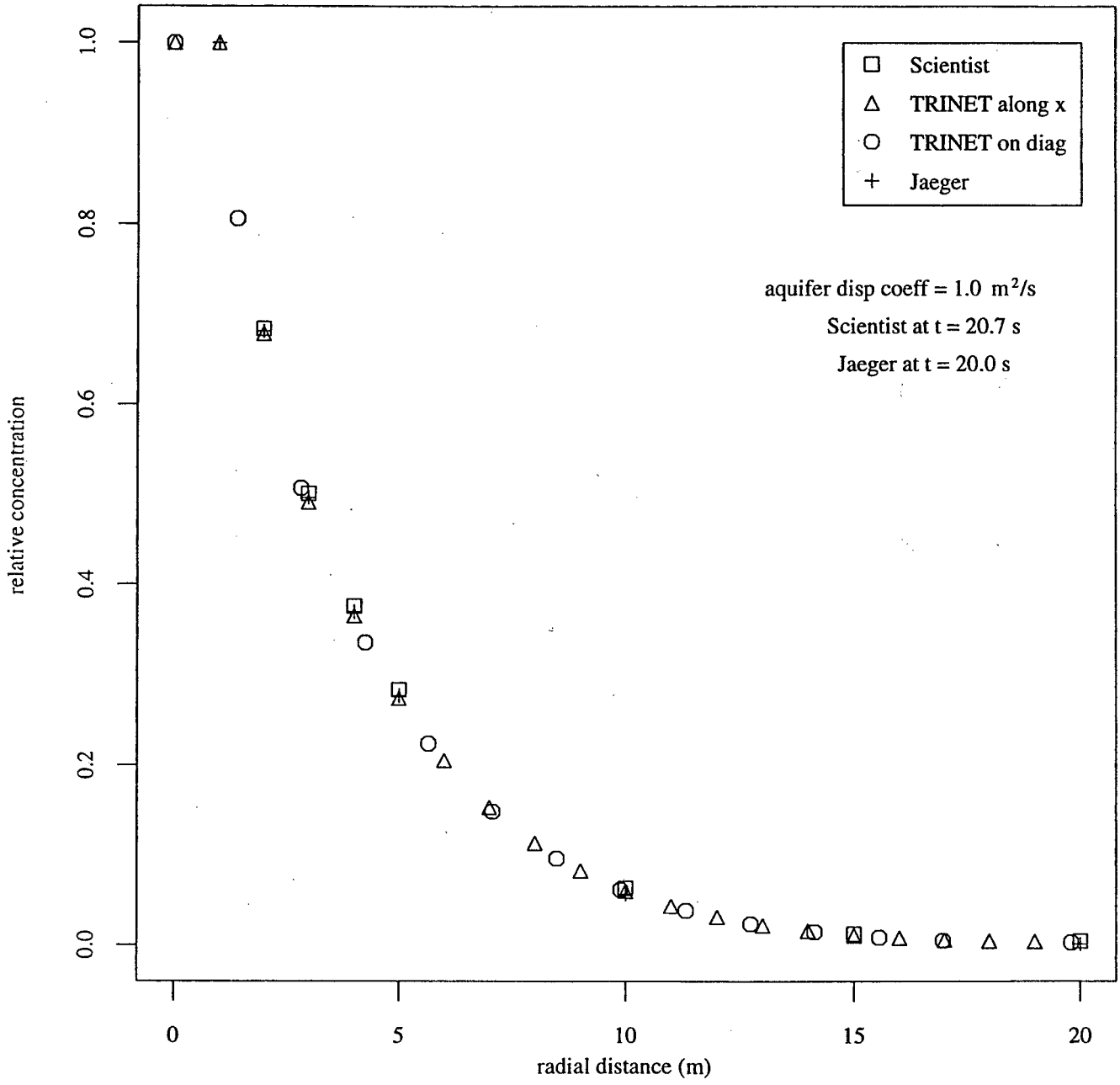

Fig. 20. TRINET comparison to analytical solution given by Jaeger [1956] and Scientist program for the diffusion-only case at TRINET time step t = 21.4 s.

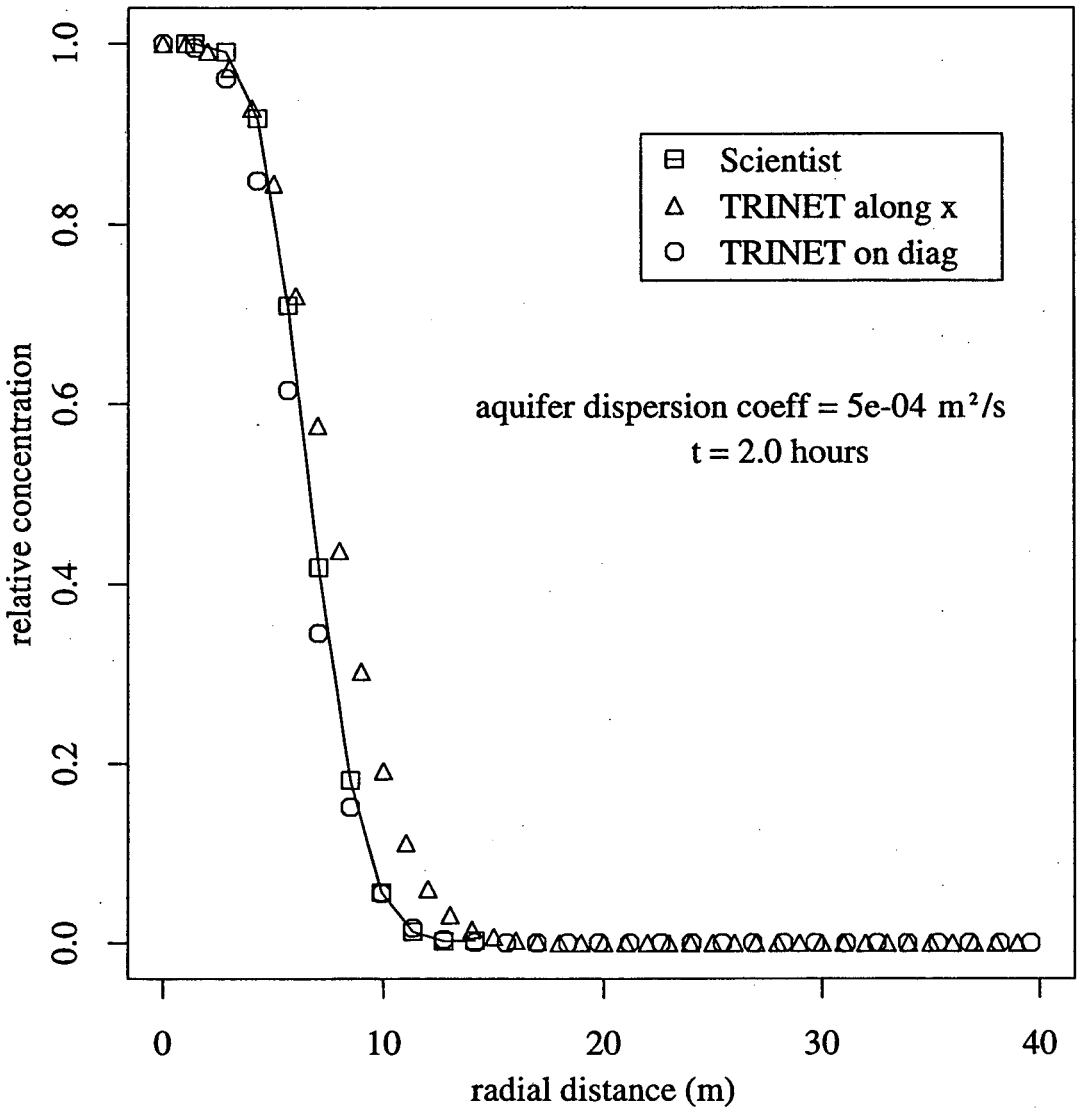

Fig. 21a. TRINET comparison to Scientist solution at early time for the case with moderate dispersion using the quarter lattice.

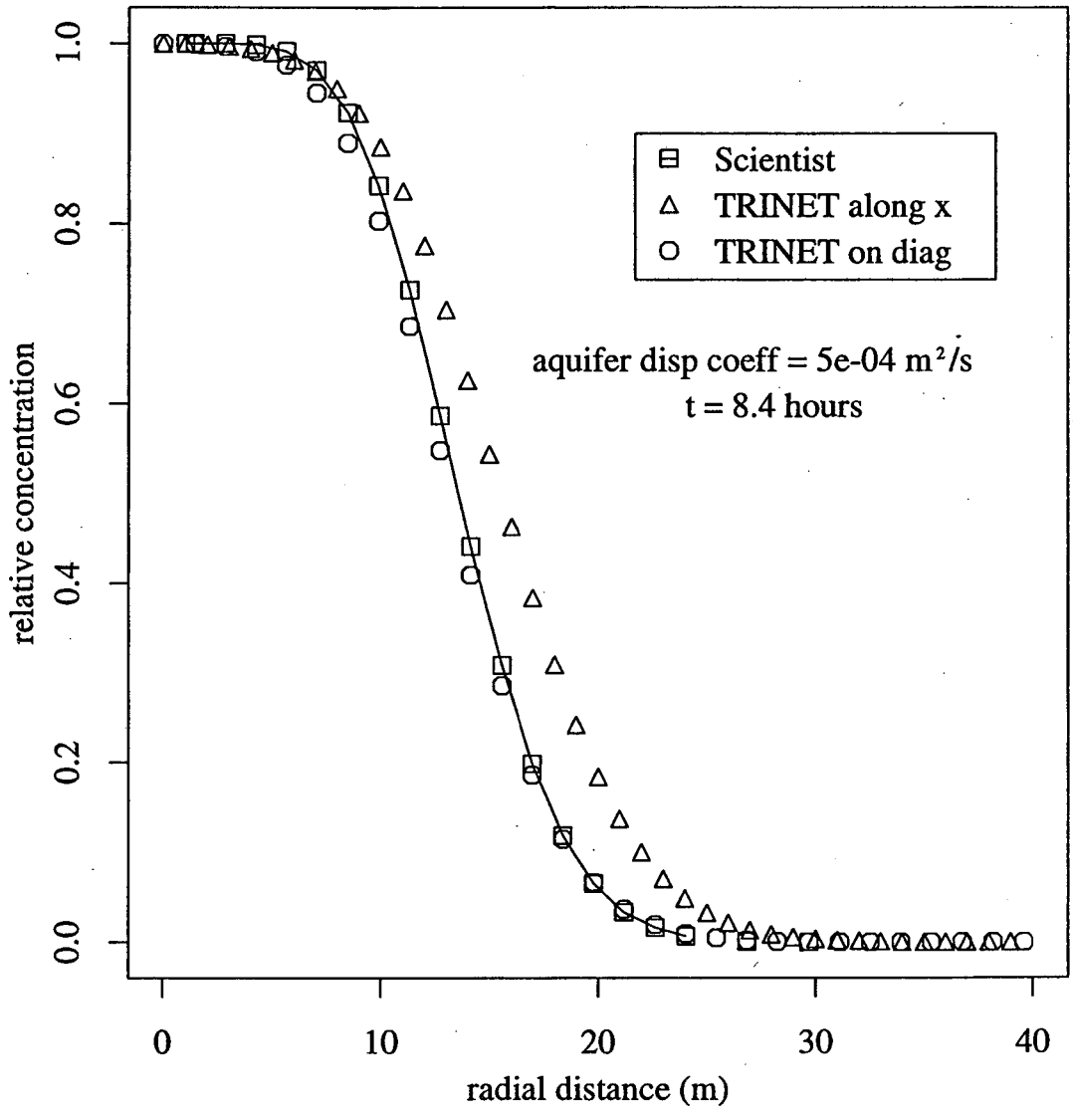

Fig. 21b. TRINET comparison to Scientist solution at middle time for the case with moderate dispersion using the quarter lattice.

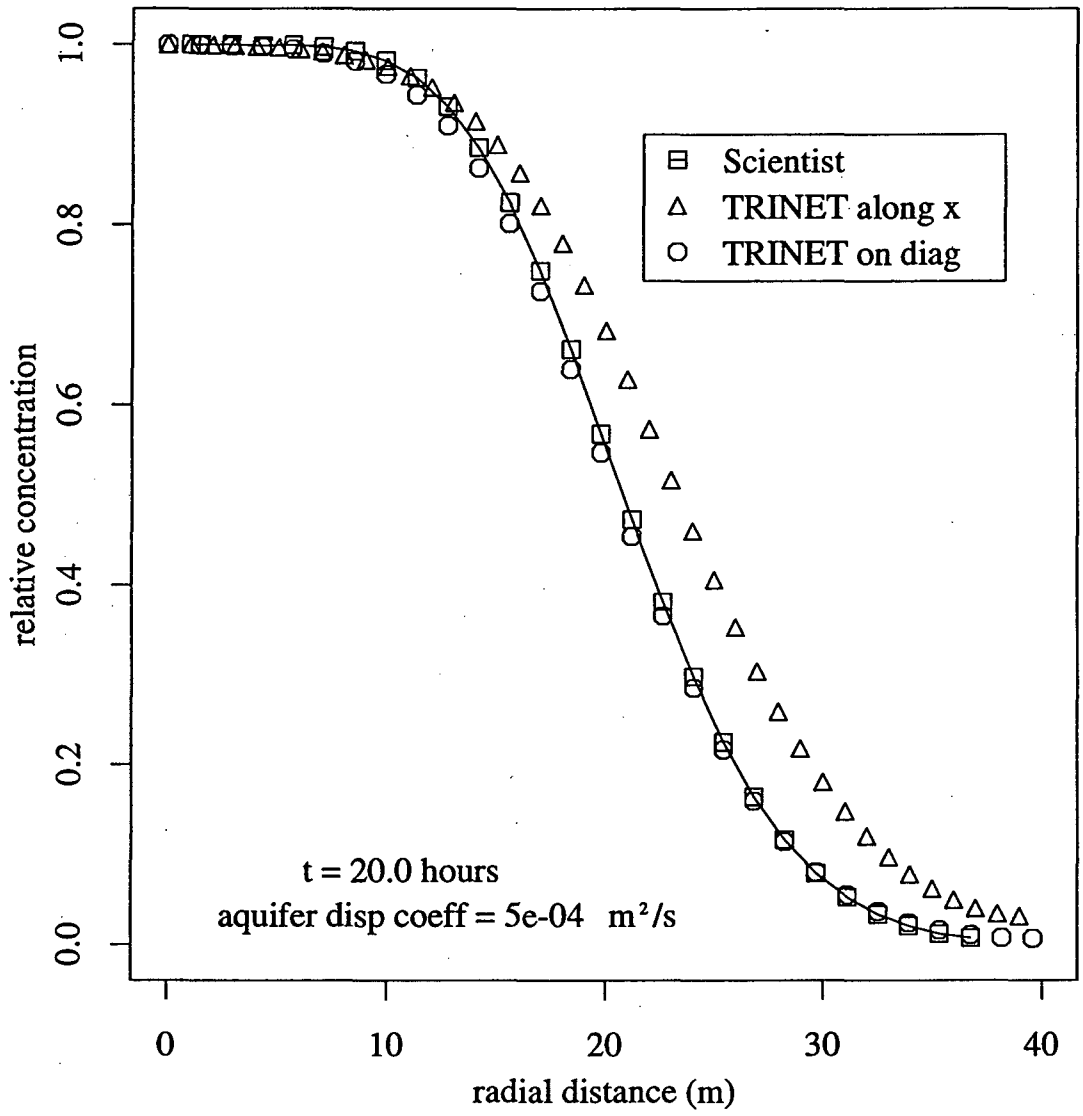

Fig. 21c. TRINET comparison to Scientist solution at late time for the case with moderate dispersion using the quarter lattice.

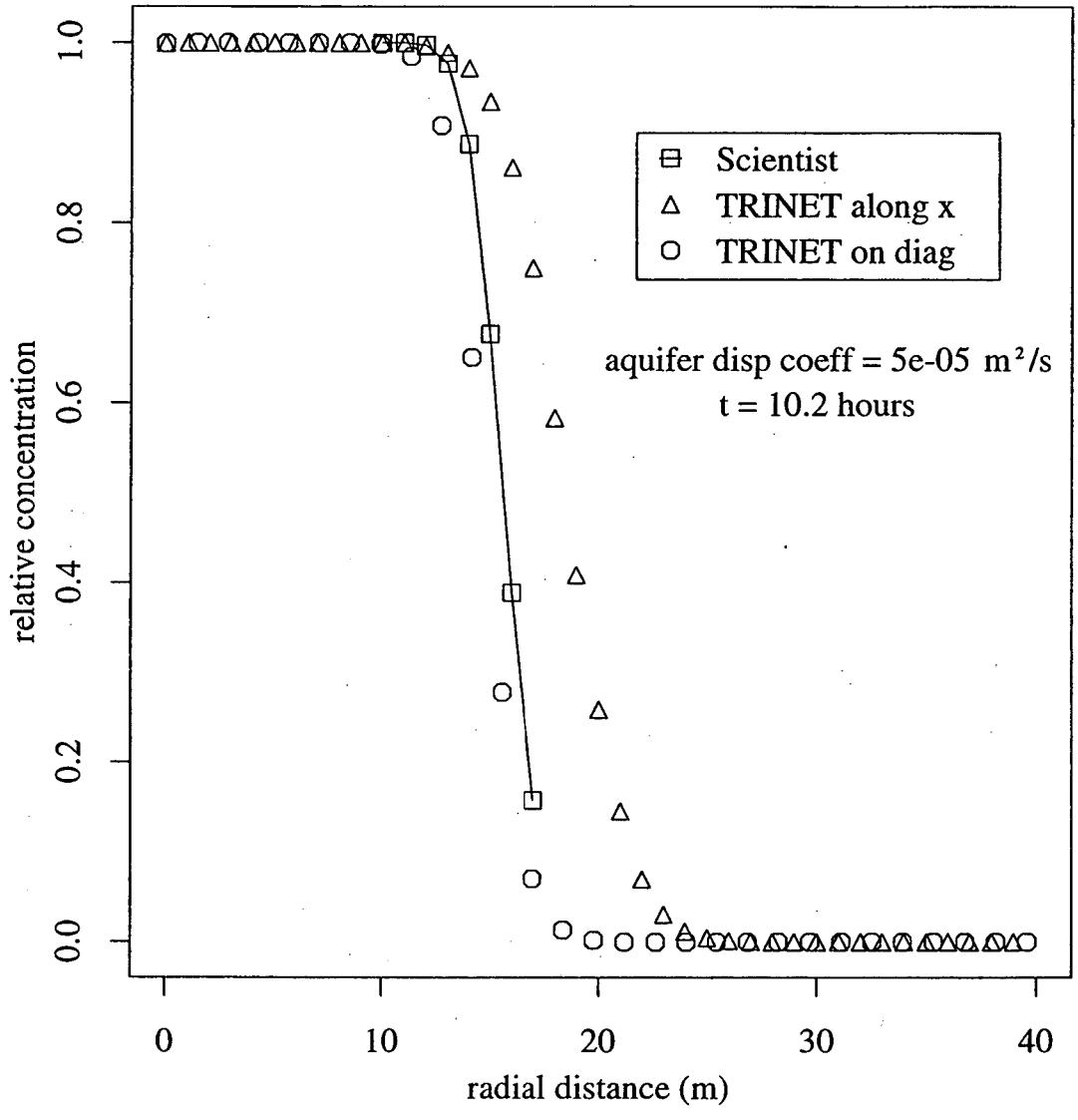

Fig. 22a. TRINET comparison to Scientist solution at early time for the case with small dispersion using the quarter lattice.

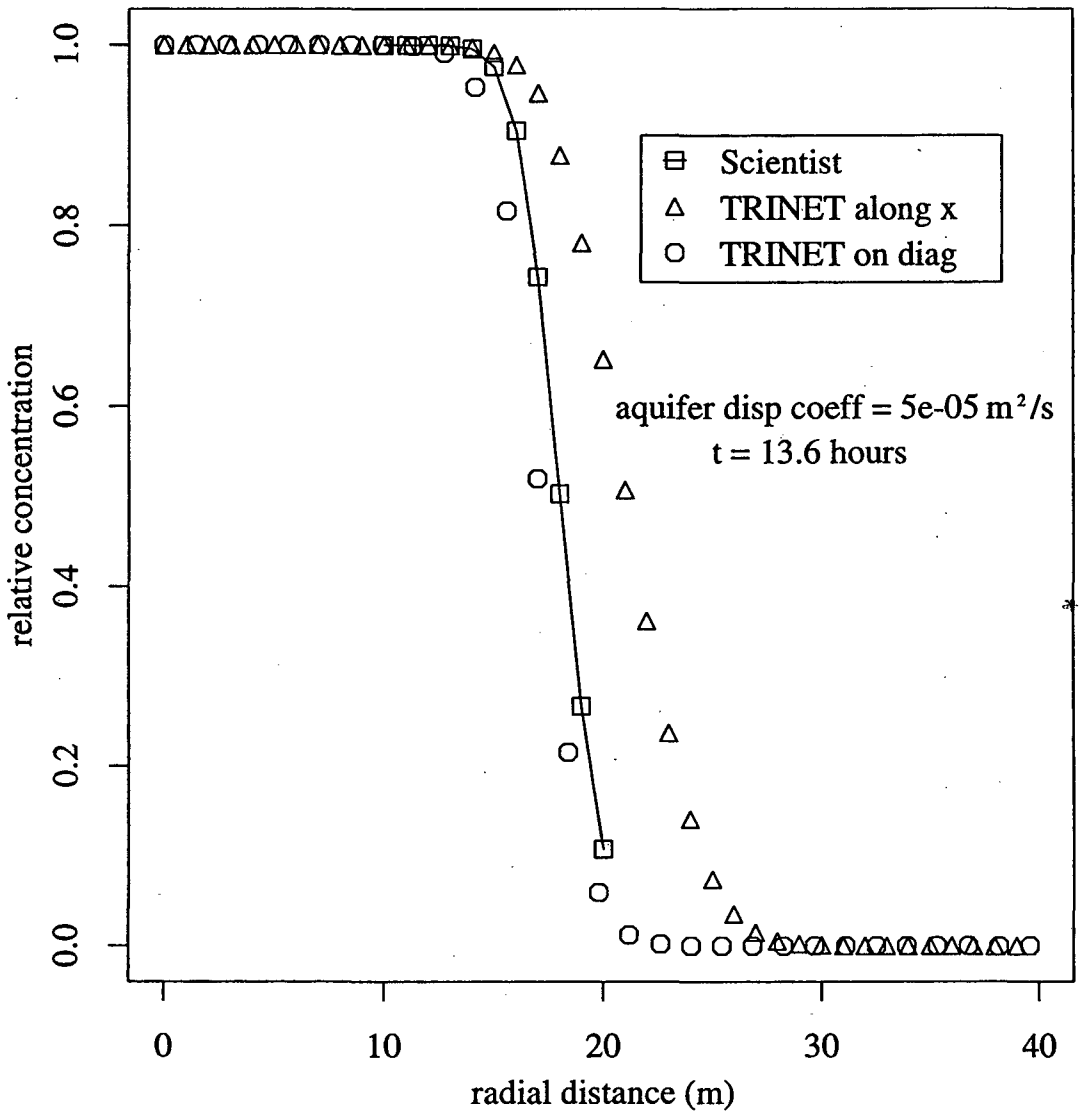

Fig. 22b. TRINET comparison to Scientist solution at middle time for the case with small dispersion using the quarter lattice.

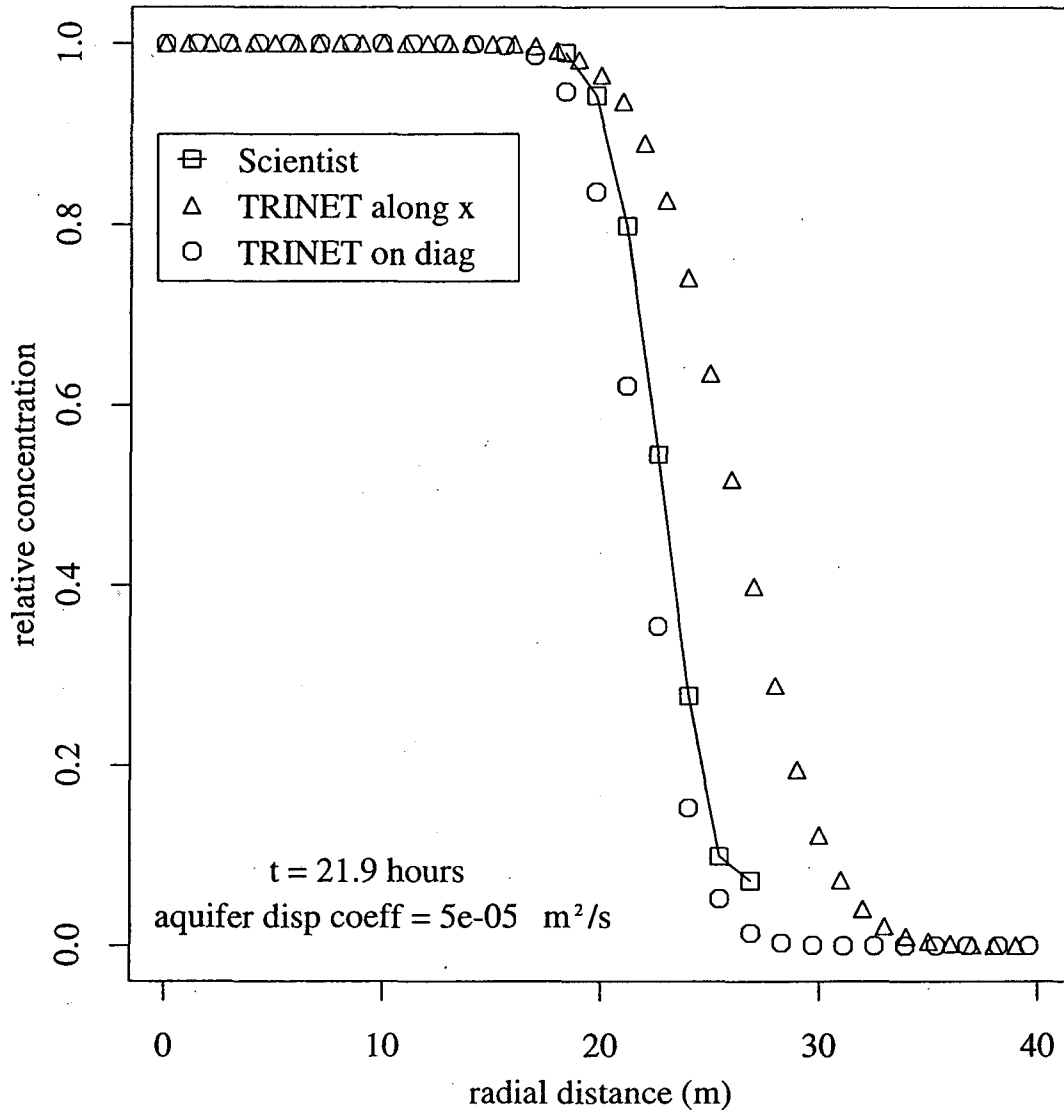

Fig. 22c. TRINET comparison to Scientist solution at late time for the case with small dispersion using the quarter lattice.

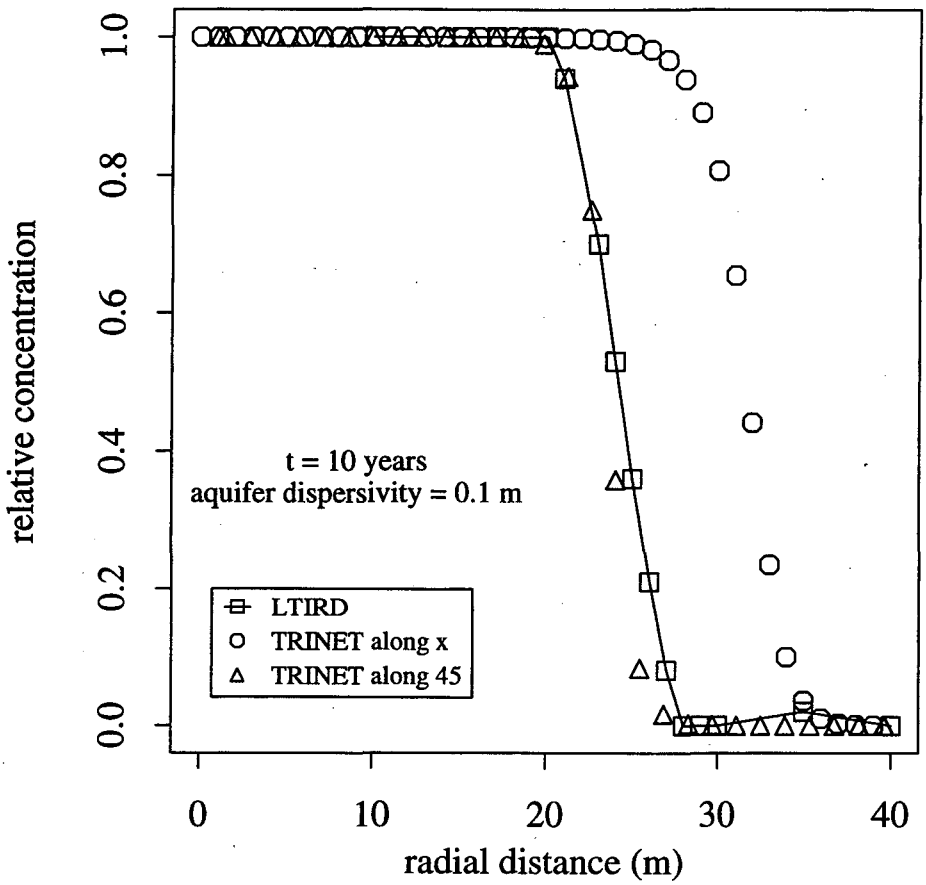

Fig. 23. TRINET comparison with LTIRD solution for the radial transport problem with a small longitudinal dispersivity using the quarter lattice.

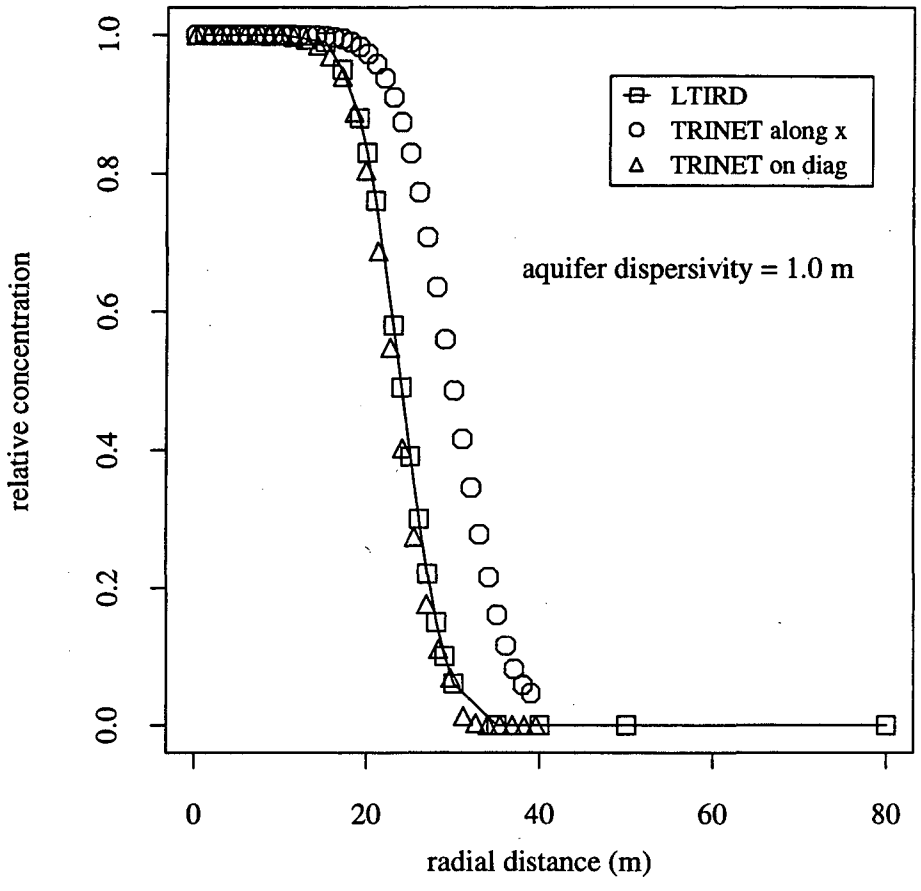

Fig. 24. TRINET comparison with LTIRD solution for the radial transport problem with a moderate longitudinal dispersivity using the quarter lattice at 10 years.

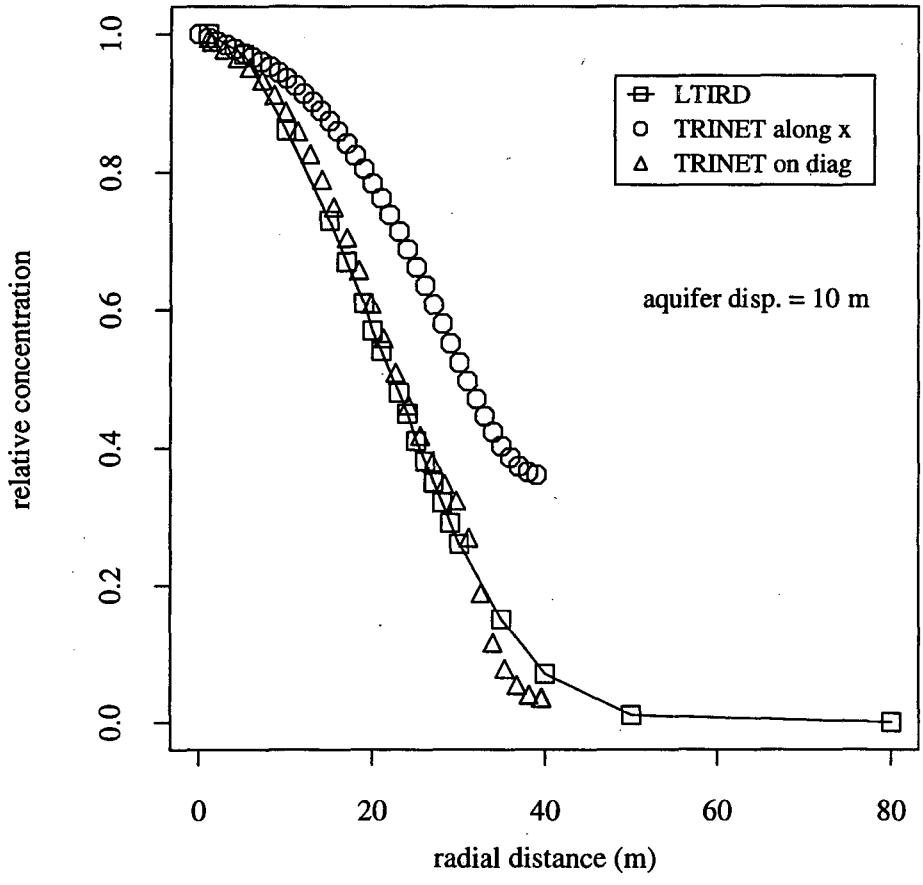

Fig. 25. TRINET comparison with LTIRD solution for the radial transport problem with a large longitudinal dispersivity using the quarter lattice at 10 years.

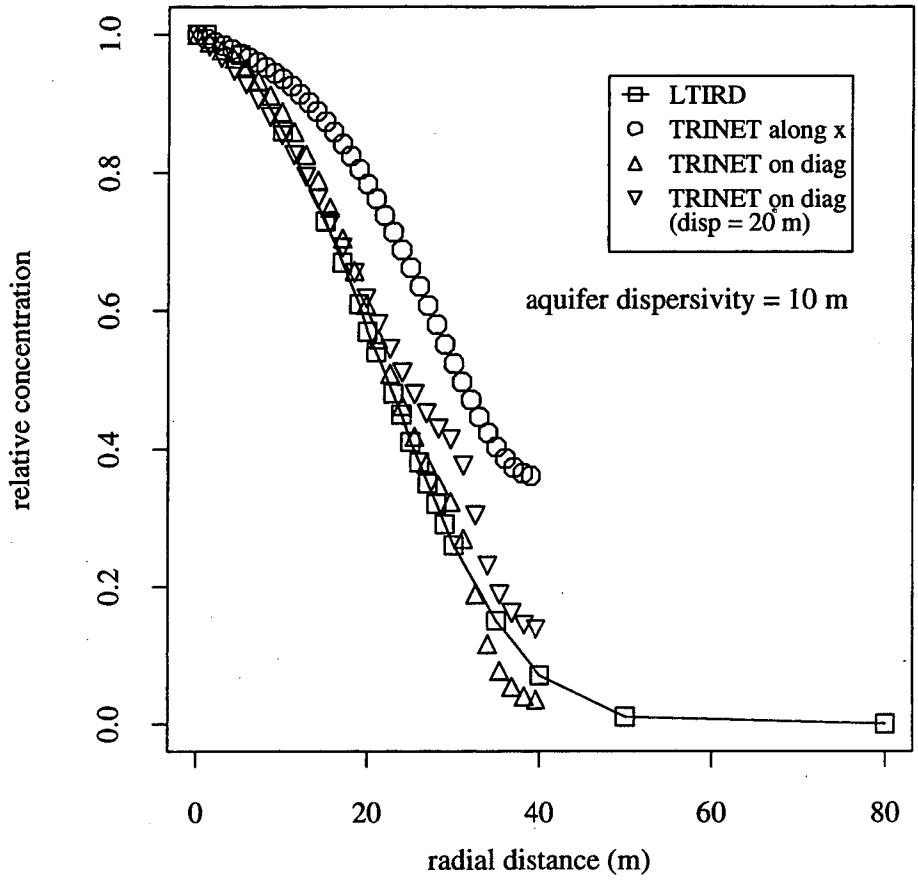

Fig. 26. TRINET comparison with LTIRD solution for the radial transport problem with TRINET element dispersivities of 10m and 20m using the quarter lattice at 10 years.

Ernest Orlando Lawrence Berkeley National Laboratory
One Cyclotron Road | Berkeley, California 94720

Prepared for the U.S. Department of Energy under Contract No. DE-AC03-76SF00098